Canadian Journal of
Zoology
Revue canadienne de
zoologie

Ionic regulation and shell mineralization in the bivalve Anodonta cygnea following heavy metal exposure

SCHOLARONE™
Manuscripts

1 **Ionic regulation and shell mineralization in the bivalve**

2 ***Anodonta cygnea* following heavy metal exposure**

3

4 **Abstract**

5 Freshwater mussels are one of the most imperiled faunistic groups in the world

6 and environmental exposure to toxic heavy metals, which result in deregulation

7 of calcium absorption and deposition in the laboratory, may be a contributing

8 factor in their decline. To address potential effects of heavy metal exposure on

9 calcium transport and metabolism in freshwater bivalves, adult *Anodonta*

10 *cygnea* L., 1758 were exposed to a sub-lethal concentration (1.0×10^{-6} M) of

11 essential (Zn^{2+} and Cu^{2+}) or non-essential (Pb^{2+} and Cr^{3+}) metal for 30 days in

12 the laboratory. Inorganic composition of extrapallial, haemolymph, heart and

13 pericardium fluids and kidney tissue, as well as shell morphology by SEM were

14 compared in treated and untreated mussels. Calcium levels in fluids varied after

15 exposure to any of the metals investigated, although the magnitude and

16 threshold of effect were metal- and compartment-specific. Ca^{2+} levels increased

17 robustly in all fluids following exposure to Zn^{2+}, Cu^{2+} or Cr^{3+}, while levels

18 decreased significantly in heart fluid alone following Pb^{2+} exposure ($p<0.05$).

19 Contrarily to the other metals exposure, Cu^{2+} revealed an interesting reverse

20 accumulation pattern decreasing in the fluids but not in the kidney, where it

21 clearly accumulates for excretion. In addition, while essential $Cu^{2+,}$ and Zn^{2+} are

22 closely regulated, the non-essential metals, Pb^{2+} and Cr^{3+}, increase to very high

23 levels. Drastic alterations in shell morphology, specifically the structure of

24 border and inner pallial regions of the nacreous layer, were observed after Cu^{2+}

25 or Cr^{3+} exposure. Collectively, data suggest that prolonged exposure to a sub-

26 lethal concentration of these heavy metals can adversely affect compartmental

27 calcium availability and shell composition in *A. cygnea*.

28

29 **Keywords**: Freshwater mussels; calcium metabolism; heavy metals; *Anodonta*

30 *cygnea; osmolarity*

31

32 **Introduction**

33 Freshwater mussels, also known as unionids or naiads, have significant

34 ecologic and economic value, playing essential roles in aquatic ecosystems

35 (Naimo 1995), such as calcium cycling (Green 1980) and mixing of superficial

36 sediment (McCall et al. 1979). They are also a natural food source (Van der

37 Schalie and Van der Schalie 1950) and a resource for the mother-of-pearl

38 industry (Helfrich et al. 1997). However, as sedentary filter feeders that strain

39 suspended particles from the water column, mussels are at high risk of

40 exposure to a wide range of persistent, soluble, and often toxic environmental

41 pollutants.

42

43 Heavy metals are one such group of environmental toxicants, entering aquatic

44 ecosystems via effluent discharge, surface runoff, or by direct deposition of

45 solid residues (Calabrese et al. 1977). Evidence of heavy metal toxicity is

46 observable even at very low concentrations (Nriagu and Pacyna 1988; Saeki et

47 al. 1993), with the threshold of effect and physiological response dependent on

48 both the type of heavy metal and the population in question. For example, the

49 risk of heavy metal exposure is higher for benthic than for pelagic fauna (Brown

50 et al. 1996), as suspended particulate matter may bind heavy metals before

51   depositing as sediment (Linde et al. 1996), thus serving as a vehicle for long-

52   term exposure and toxicity.

53

54   Effects of heavy metal exposure have already been investigated in the

55   freshwater mussel *Anodonta cygnea* L., 1758 (Bivalvia Unionidae), and shell

56   calcification has been identified as a susceptible physiological process. In

57   particular, exposure to any of the metallic ions investigated (Cd, Zn, Cu, Al, Ni

58   and Co) at final concentration of 0.1 mM leads to an increase in shell

59   calcification, due to a variation in the ionic current of the outer mantle epithelium

60   (OME) (Moura et al. 2000, 2001; Antunes et al. 2002). Additional exposure

61   effects include metabolic acidification and subsequent dissolution of internal

62   calcareous concretions resulting in an increase in free Ca^{2+} in hemolymph

63   (Moura 2000, Antunes et al. 2002, Faubel et al. 2008); such an increase in Ca^{2+}

64   is in turn responsible for an electrochemical gradient raising Ca^{2+} diffusion into

65   the shell compartment and eventually calcium deposition(Lopes-lima et al.

66   2008). It is worth noting, however, that OME cellular activity and resultant shell

67   calcification are seasonal (Coimbra et al. 1988; Moura et al. 2000, 2001, 2003;

68   Lopes-Lima et al. 2005), and therefore any effects observed after heavy metal

69   exposure may also be influenced by seasonality.

70

71   Bivalves environmentally exposed to high concentrations of heavy metals still

72   have a high survival rate (Couillard et al. 1993), despite documented

73   physiological effects and a progressive increase in tissue burden (Hemelraad et

74   al. 1986; Jenner et al. 1991). Metal tolerance in such accumulator organisms by

75   necessity involves sequestration of metals in non-toxic forms. In bivalves, a

76   variety of sequestration sites are available and include high-affinity metal-

77   binding proteins such as metallothioneins, lysosomes, granules, calcareous

78   microspherules, and even the shell (Mason and Jenkins 1995).

79

80   The aim of the present study was to examine (i) potential effects of heavy metal

81   exposure on the levels of main ions (Ca^{2+}, Mg^{2+}, K^+, Na^+ and Cl^-), the respective

82   osmolarity and metal burden in fluids collected from extrapallial, hemolymph,

83   heart and pericardium and kidney tissue in *A. cygnea*; (ii) its influence on

84   calcium transport and absorption and (iii) deposition of calcium carbonate on

85   the morphology of inner shell layers by means of SEM evaluation.

86

87   **Methods**

88   *Animals and treatment*

89   Adult freshwater mussels, *A. cygnea* (Unionidae), were collected from Mira

90   Lagoon in Northern Portugal and acclimated for 24 hours in aerated tanks

91   containing dechlorinated water prior to treatment. A total of 25 healthy animals

92   were distributed into 5 experimental groups and housed individually (five

93   animals per group, one animal per tank). Each tank contained 10 L of

94   reconstituted water (Coimbra and Machado 1988) at a final concentration of 1.0

95   x 10^{-3} M $CaCl_2$. Animals were considered healthy when they showed active

96   ventilation, powerful valve closing or water ejection upon disturbance, and a

97   smooth and shiny nacreous shell layer.

98

99   Each experimental group was treated with one of the following heavy metals for

100   30 days at a final sub-lethal concentration of 1.0 x 10^{-6} M: Cu^{2+} ($CuSO_3$), Pb^{2+}

101 (PbCl$_2$), Zn^{2+} (ZnSO$_3$•7H$_2$O), Cr^{3+} (CrCl$_3$•6H$_2$O). The control group remained

102 untreated.

103 Every other day animals were fed a microalgae suspension of cultured *Chlorella*

104 spp. and *Ankistodesmus* spp. (10.0 x 10^7 cells/mL) (Faubel et al. 2008) for 2

105 hours in a separate tank. After this procedure, the water in each treatment tank

106 was replaced.

107

108 *Sample collection*

109 At the end of the 30-day experimental period, animals were sacrificed by

110 immersion in 4 mL/L 2-phenoxyethanol solution (Sigma-Aldrich, Munich**,**

111 Germany) for 20-30 minutes (Ngo et al. 2010a). Fluid from the extrapallial

112 (between the shell and mantle), mantle (between both mantle epithelia), heart,

113 and pericardial compartments were immediately collected using a 21-gauge

114 needle (0.80 x 40 mm; Braun Sterican) attached to a sterile syringe, as

115 described by Morton (1983). Fluid samples were immediately processed; the

116 total volume of fluid extracted from each anatomical compartment

117 (approximately 5 mL) was placed into a 14-mL acid-washed centrifuge tube and

118 stored on ice until centrifuged at 4500 rpm for 7 min. The supernatant was then

119 transferred to a second acid-washed tube and stored at -20ºC until analysed.

120 Kidney tissue samples were also collected and weighed immediately prior to

121 processing; tissue was then placed in an Eppendorf tube containing 50 µL of

122 Ultra Pure water, centrifuged to remove debris, and transferred to another

123 Eppendorf tube prior to storage at -20ºC until analysis. Shell samples from each

124 bivalve shell (a total of 10 samples per group) were collected using a diamond

125 saw at the same anterior-posterior distance (3 cm), radially in the direction of

126 the umbo.

127

Ion quantification

129 Fluid samples were thawed and resuspended in a 0.6 M HNO_3 solution to a final

130 volume of 4 mL. Kidney tissue samples were thawed, then dried for 2 hours at

131 60ºC prior to digestion with 0.6 M HNO_3 at high pressure using a Parr

132 microwave acid digestion bomb, (Model 4782; Moline, IL, USA). Na^+ and K^+

133 levels were determined by atomic emission spectrometry. Ca^{2+}, Mg^{2+} and Zn^{2+}

134 levels were determined by atomic absorption spectrometry with an atomization

135 flame detector. Cu^{2+}, Pb^{2+} and Cr^{3+} levels were determined by electrothermal

136 (graphite chamber) atomic absorption spectrometry using a Varian (Palo Alto,

137 CA, USA) SpectrAA 220 FS Atomic Absorption Spectrometer. Procedures used

138 for the quantification of inorganic elements in experimental samples were first

139 validated with concentration standards (Fluka, Pro analysis) and SRM 2976

140 ("Mussel Tissue") as reference material. Cl^- concentration was determined by

141 coulometric titration using a Jenway Model PCLM3 automatic chloride meter

142 (Felsted, England). Fluid osmolarity was determined by the freezing depression

143 method using a Loser Messtechnik Type 15 automatic micro-osmometer

144 (Berlin, Germany).

145

Statistical analysis

147 For each parameter studied, data was tested for normality, and square-root

148 transformed if necessary. Means were then analyzed by one-way analysis of

149 variance (ANOVA) using SPSS v12.0 for Windows, followed by a posthoc

150   Dunnett's test for multiple comparisons when applicable. Statistical significance

151   was set at $p<0.05$.

152

153   *Scanning electron microscopy*

154   Individual shell fragments were mounted on scanning electron microscopy

155   (SEM) specimen stubs with conductive silver paint and then coated with gold.

156   The inner surface of the nacreous layer was then examined through a JEOL

157   JSM-35C scanning electron microscope operated at 25K.

158

159   **Results**

160   *Heavy metal exposure alters fluid ion levels in the body*

161   Concentrations of individual electrolytes Ca^{2+}, Mg^{2+}, Na^+, Cl^-, K^+ in *A. cygnea*

162   were quantified in extrapallial, haemolymph, heart, and pericardium fluids, as

163   well as kidney tissue in untreated controls and after prolonged exposure to

164   Cu^{2+}, Pb^{2+}, Zn^{2+} and Cr^{3+} (Tables 1-4).

165

166   Effects of heavy metal exposure on fluid Ca^{2+} and Mg^{2+} levels were

167   dependent on both the heavy metal investigated and the anatomical location of

168   sample collection (Figs.1 and 2). Mussels exposed to both essential (Cu^{2+}, Zn^{2+})

169   and non-essential (Cr^{3+}) ions, usually showed increased Ca^{2+} and Mg^{2+} levels,

170   as compared to untreated controls in all fluid compartments examined, mainly

171   under Cu^{2+} and Cr^{3+} treatments where calcium and magnesium contents were

172   significantly changed ($p<0.05$), respectively. While Mg^{2+} had a slight increase in

173   all fluids after exposure to Pb^{2+}, Ca^{2+} levels significantly decreased ($p<0.05$)

174   mainly in the heart.

175

176   Exposure to Cu^{2+}, Pb^{2+}, Zn^{2+} and Cr^{3+} heavy metals generally reduced

177   K^+ levels in fluid samples, when compared to the control (Fig. 3), mainly under

178   Pb^{2+} treatment, in which case K^+ concentration significantly decreased in all

179   fluid compartments ($p<0.05$). Similarly, a reduction in Na^+ (Fig. 4) and Cl^- (Fig.

180   5) concentrations in fluid samples were observed to varying extents after heavy

181   metals exposure, relative to untreated controls. Mainly, exposure to Cu^{2+} elicited

182   a very clear significant decrease in both Na^+ and Cl^- levels in major fluid

183   samples examined ($p<0.05$).

184

185   *Heavy metal exposure alters hemolymph osmolarity*

186   Osmolarity, which reflects the sum of Na^+, Cl^- and Ca^{2+} levels, was reduced to

187   varying extents in fluid samples collected from all anatomical locations following

188   heavy metal exposure, as compared to untreated controls. The only exception

189   was the extrapallial fluid following Zn^{2+} exposure, which remained unchanged

190   (Fig. 6). Although Cr^{3+} exposure resulted in significant reductions in osmolarity

191   in all fluid samples examined ($p<0.05$), for the other heavy metals investigated

192   significance was limited to the pericardium, in response to either Cu^{2+} or Pb^{2+}

193   exposure ($p<0.05$).

194

195   *Heavy metal burden in treated mussels*

196   The content of heavy metals within compartment fluid and kidney tissue

197   samples of experimental treatment groups was also assessed (Table 5).

198   Though not significantly, Cu^{2+} content (Fig. 7) was reduced in every

199   compartment except in the kidney, where it slightly increased after Cu^{2+}

200   exposure. In contrast, Zn^{2+} levels increased in all fluids after exposure, with the

201   exception of a small decrease in the kidney (Fig. 8). The most relevant effects

202   were observed in Pb^{2+} (Fig. 9) and Cr^{3+} (Fig. 10) contents, which rose

203   considerably ($p<0.05$) in all compartments in each exposure group, when

204   compared to untreated controls.

205   Curiously, when compared to the other metal (Zn^{2+}, Pb^{2+} and Cr^{3+})

206   exposure experiments, Cu^{2+} induced a reverse accumulation pattern in the

207   extrapallial, hemolymph, heart and pericardium fluids.

208

209   *Heavy metal exposure alters shell morphology*

210   SEM images of the inner layer of *A. cygnea* bivalve shells revealed differences

211   in morphology and calcium carbonate crystal formation following heavy metal

212   exposure.

213

214   *Untreated mussels*

215   Micrographs of shells from untreated controls (Fig. 11) presented the normal

216   morphologic features and structural characteristics of the *A. cygnea* bivalve

217   shell. As can be seen in Fig. 11.1, the prismatic layer has a regular polygonal

218   arrangement with joined calcium carbonate crystals (magnified in Fig. 11.2).

219   Towards the interior, a transition zone comprised of an emerging nacreous layer

220   and 3-4 layers of unconnected rounded crystals undergoing simultaneous

221   formation was observable (Fig 11.3), although these crystals started to lose

222   their rounded shape and tended to become rhombohedral (Fig. 11.5). More

223   polyhedric crystals, a co-existence of hexagonal and rhombohedral shapes,

224   were observed closer to the pallial line (Fig. 11.6). Adjacent to the sinuous

225   pallial line made up of crystals of undefined structure (Fig. 11.7), the nacre

226   revealed increased crystal production with high organic matrix content, which

227   yielded a less defined crystal shape (Fig. 11.8 and 11.9).

228

229   *Mussels exposed to heavy metals*

230   Micrographs of shells from mussels exposed to heavy metals illustrate

231   morphologic and structural changes in *A. cygnea* (Fig. 12 and 13). Whereas

232   bivalve shells from animals treated with Pb^{2+} (Fig. 12.1-12.4) or Zn^{2+} (Fig. 13.1-

233   13.4) were morphological indistinguishable from controls, micrographs of shells

234   from mussels exposed to Cu^{2+} revealed substantial morphological changes (Fig.

235   14.1-14.4). As shown in Fig. 14.1, the prismatic layer presented a normal

236   arrangement, except for an accelerated precipitation of small crystals. Further

237   magnification revealed the presence of shattered crystals at the origin of the

238   nacreous layer, resulting in an irregular exterior shape that is not present

239   among untreated controls (Fig. 14.2). Inward of the sinuous pallial line (Fig. 14.3

240   and 14.4) several unconnected layers, up to ten crystal-layers thick, formed

241   deeper grooves in shells from Cu^{2+} exposed animals.

242   SEM images of shells from animals exposed to Cr^{3+} exhibited a similar though

243   more pronounced pattern than those exposed to Cu^{2+} (Fig. 15); in particular,

244   newly formed prismatic crystals were greater in number (Fig. 15.1) and had a

245   granulous shape. This pattern was also evident in the nacreous layer (Fig.

246   15.2), where very rapid precipitation was observed, especially on the edges of

247   rhombohedral crystals. Interior to the pallial line (Fig. 15.3 and 15.4), the

248   grooves were deeper in shells from Cr^{3+} exposed animals, thus revealing the

249   formation of multiple unconnected layers.

250

Discussion

Surprisingly little is known of the mechanisms ruling calcium absorption in mollusks, despite its established importance in cellular signaling, exoskeleton formation, and larval development (Moura et.al. 1999, 2004). However, research on the freshwater mussel *A. cygnea* has suggested that ionic pathways such as those involved in shell calcification are susceptible to heavy metal interference (Moura et.al. 2000, 2001), which calls for further research on ion equilibrium in the face of metal exposure. After studying the potential effects of prolonged exposure to essential and non-essential heavy metals in *A. cygnea,* the findings described in this paper, include significant variations in individual ion levels and osmolarity, as well as heavy metal-specific effects, such as heavy metal burden in an exhaustive fluid panel and kidney tissue samples. Clear changes in shell morphology at the prismatic and nacreous layers are also observable after exposure to Cu^{2+} or Cr^{3+}, but not Pb^{2+} or Zn^{2+}.

Calcium requirements of freshwater mussels are satisfied by both dietary intake (Van Der Borght and Van Puymbroeck 1966) and active transport from their hypocalcemic environment (Schoffenkls 1951; Jodrey 1953; Kado 1960; Van Der Borght 1962, 1963). Though little is known about the mechanism of calcium absorption in either marine or freshwater mollusks, calcium ions can be stored in transient calcareous deposits (microspherules) in the mantle and gills (Machado et al. 1988). Heavy metals, which have been shown to impact calcium metabolism and transport, mainly by competing for binding sites (Antunes et al. 2002), also accumulate in the mantle and gills (Manly and

275   George 1977). It must be pointed out that heavy metal accumulation has been

276   reported in other organs and appears to be metal-specific, which may be a

277   result of differential metal transport in each compartment.

278

279   *Physiological ion levels following metal exposure*

280   In the course of our study, exposure to the essential heavy metals Cu^{2+} or Zn^{2+},

281   at sub-lethal concentrations, significantly or slightly raised fluid Ca^{2+} contents in

282   examined samples of extrapallial, hemolymph, heart and pericardium fluids,

283   respectively. In addition, Mg^{2+} levels rose in all fluid samples in Cu^{2+}-exposed

284   but not in Zn^{2+}-exposed mussels, thus suggesting that Cu^{2+} exposure elicits a

285   greater toxic effect than Zn^{2+}. Cu^{2+} mediated acidosis is the ultimate source of

286   fluctuations in physiological Ca^{2+} and Mg^{2+} levels and toxicity - a combined

287   result of altered respiratory function reducing oxygen levels (Rtal et al. 1996),

288   alteration in homeostatic regulation (Nonnotte et al. 1993), energy demanding

289   metal detoxification (Mason and Simkiss 1982; Moura et al. 1999, Ngo et al

290   2010b), and inhibition of carbonic anhydrase (Ngo, Gertsmann, and Frank

291   2010c). Collectively, these alterations promote overall internal acidosis, which is

292   more severe after Cu^{2+} than Zn^{2+} exposure. Internal acidosis, in turn, results in

293   dissolution of calcium microspherules in the gills and mantle (Machado et al.

294   1988; Moura et al. 1999, Moura 2000, Antunes et al. 2002, Faubel et al. 2008)

295   and the eventual release of Ca^{2+} and Mg^{2+} into the hemolymph. Indeed, the

296   data provided in this paper show proportional increases in Ca^{2+} and Mg^{2+}

297   relative to the toxicity of the metal, in accordance with the literature. However,

298   with the exception of Cr^{3+} exposed mussels, this trend was not observed in the

299   kidney tissue.

300   Conversely, exposure to non-essential heavy metals (Cr^{3+}, Pb^{2+}), at sub-

301   lethal concentrations, elicited metal-specific effects on physiological Ca^{2+} and

302   Mg^{2+} levels in extrapalial, hemolymph, heart and pericardium fluids. Although

303   Cr^{3+} treatment elicited effects similar to Cu^{2+} (clearly raising Ca^{2+} and Mg^{2+}

304   levels, most likely through metabolic acidosis (Machado et al. 1988; Jeffree et

305   al. 1993, Moura et al. 1999.)) effects associated with Pb^{2+} treatment were

306   mainly limited to a decline in Ca^{2+} levels in the fluid collected from the heart.

307   Simons (1986) and Yücebilgiç et al. (2003) have shown that Pb^{2+} exposure

308   disturbs Ca^{2+} transport, and a similar mechanism may be at work in *A. cygnea*.

309   This very specific effect on the heart, in combination with others using vitamin D

310   as a calcium movement promoter and SEA0400 as inhibitors of calcium

311   transport (Faubel et al. 2008), may indicate an active calcium uptake from the

312   gastrointestinal tract and resorption from the pericardium to the heart (Fig. 16).

313   Therefore, any calcium content excess in heart fluid, e.g. after Cd^{2+} exposure

314   (Faubel et al. 2008), might be transported towards the pericardium and kidney

315   excretion pathway by diffusion in the heart epithelium (Fig. 17).

316

317   *Osmolarity, K^+ Na^+ and Cl^- ion levels following heavy metal exposure*

318   It is worth pointing out that heavy metal exposure, including the essential metals

319   Zn^{2+}, Cu^{2+} and Cr^{3+}, reduced Na^+, Cl^- and K^+ levels, when compared to

320   untreated controls from samples of extrapallial, hemolymph, heart pericardium

321   fluids. This decrease may work as a compensatory mechanism in order to

322   maintain internal osmolarity, thus making up for increases in Mg^{2+} and Ca^{2+}

323   ionic concentrations. The significant reduction in osmolarity in all fluids after Cr^{3+}

324   exposure, despite a rise in physiological Ca^{2+} and Mg^{2+} levels, is indicative of

325   the high toxicity of this metal, as well as of the compensatory effect of reduced

326   Na^+ and Cl^- levels. In contrast, osmolarity was unaffected by Pb^{2+} exposure,

327   suggesting that Pb^{2+} is less toxic than Cr^{3+}. In view of the small changes in

328   physiological Ca^{2+} and Mg^{2+} levels following Pb^{2+} exposure, and in spite of the

329   dramatic changes in Na^+, K^+, and Cl^- ions in all fluids, ionic regulation may

330   depend on elements other than those investigated in the present study, such as

331   bicarbonate, phosphate or sulfate ions.

332

333   *Heavy metal burden*

334   Whereas levels of essential trace metals, such as Zn^{2+} and Cu^{2+}, are to

335   some extent regulated (Simkiss and Mason 1983), concentrations of non-

336   essential metals, such as Pb^{2+} and Cr^{3+}, are dependent solely on environmental

337   concentrations and bioavailability, although some degree of regulation is

338   possible (Dalinger and Weiser 1984).

339   In the course of our study, we determined that exposure to sub-lethal

340   concentrations of the essential metals Zn^{2+} and Cu^{2+} for 30 days did not

341   significantly alter their concentration in the extrapallial, hemolymph, heart and

342   pericardium fluids and kidney tissue. However, inverse pattern trends were

343   observed in the same compartments following Zn^{2+} or Cu^{2+} exposure. While

344   Zn^{2+} increased in samples collected from all compartments, with the exception

345   of kidney, Cu^{2+} decreased in samples collected from all compartments, with the

346   exception of kidney, where it increased. The data suggest that Zn^{2+} forms a

347   gradient from the heart through the mantle towards the extrapallial

348   compartment, mirroring the flow of hemolymph within the open circulatory

349   system (illustrated in Fig. 17). Our hypothesis is supported by the observations

350   of Moura et al. (1999), who reported that Zn^{2+} exposure in *A. cygnea* elicited an

351   increase in Zn^{2+} deposits within the shell's nacreous layer, and of Meites (1964)

352   and Pietrzak et al. (1976), who concluded that Zn^{2+} first precipitates in the

353   mineral structures (shell and/or microspherules) due to a lower solubility than

354   that of the calcium carbonate. The inverse gradient observed following Cu^{2+}

355   exposure suggests that the metal is excreted by the kidney. Higher Cu^{2+} content

356   in the kidney, as compared to pericardial fluid, is likely a result of Cu^{2+}

357   accumulation prior to excretion. Notably, Cu^{2+} exposure in bivalves induces

358   expression of metallothioneins in kidney (Choi et al. 2003).

359

360   Exposure to the non-essential heavy metals Pb^{2+} or Cr^{3+} resulted in significant

361   increases in Pb^{2+} or Cr^{3+} contents in all sampled compartments, when

362   compared to untreated controls, which had very low or undetectable levels.

363   Though Pb^{2+} exposure resulted in a high accumulation of Pb^{2+} in fluid from

364   heart, mantle and extrapallial compartments favoring an excretory pathway to

365   the extrapallial compartment and shell, Cr^{3+} levels were higher in fluid from the

366   pericardium and kidney tissue, which favors an alternative excretory pathway.

367   These data suggest that the Pb^{2+} gradient, which initiates in the heart and

368   progresses through the mantle towards the extrapallial compartment in

369   accordance with the flow of the circulatory system (Fig 16), is predictive of

370   precipitation within the shell. Moura et al. (2001) reported that the shell was the

371   main Pb^{2+} detoxification target. Moreover, even with strong accumulation on all

372   compartments, there was no detectable metabolic acidosis effect (unchanged

373   calcium and magnesium levels). In fact Black et al. (1996) had already found

374   that Pb^{2+} tissue concentration was poorly correlated with adverse effects on

375   *Anodonta grandis*. Conversely, as in Cu^{2+} exposure, the observed Cr^{3+} gradient,

376   which peaks in the kidney, is indicative of posterior excretion via the kidney. Our

377   hypothesis is supported by the findings of Walsh and O'Halloran (1998) and

378   Boening (1999), which suggested this organ as the main detoxification pathway

379   for Cr^{3+}.

380

381   *Shell morphology following heavy metal exposure*

382   In accordance with the toxicity data in soft tissue presented here, structural

383   changes in the shell, border, pallial and inner zones were observed following

384   exposure to Cu^{2+} but not Zn^{2+}, possibly due to the metabolism of organic

385   compounds involved in the biomineralization phenomena. Interestingly, the

386   deep grooves observed on the inner shell layer were similar to alterations

387   induced by Diflubenzuron, a benzamide insecticide. This similarity might be

388   related to changes in chitin polymerization (Machado et al**.** 1991), which would

389   in turn compromise the framework matrix.   The interruption of this organic

390   framework by Cu^{2+} action, most likely due to a disruption of chitin

391   polymerization, induced several unconnected calcareous lamina that formed

392   grooves in the nacreous layer.

393

394   Exposure to the non-essential heavy metals Pb^{2+} or Cr^{3+} produced differential

395   effects on the formation of the nacreous layer. When compared to untreated

396   controls, Pb^{2+} exposure failed to elicit structural changes, whereas Cr^{3+}

397   exposure generated visible effects, including deep groove formations in the

398   shell structure. This suggests a strong disturbance of cellular metabolism,

399   similar to that obtained with Cu^{2+}, although the extent of the Cr^{3+} effect was

400   greater. As mentioned above, such features indicate an alteration in the chitin

401   polymerization mechanism and a subsequent change in the properties of the

402   organic matrix framework, which interfere with normal $CaCO_3$ crystal

403   mineralization (Machado et al. 1991). Although Pb^{2+} burden was significantly

404   higher than Cr^{3+} in anatomical compartments, and the Pb^{2+} excretion pathway is

405   most likely through the shell, no shell structural alterations were evident in Pb^{2+}

406   exposed mussels. Conversely, Cr^{3+} exposure produced clear changes in the

407   nacreous layers, despite a low Cr^{3+} burden and the fact that the main

408   detoxification pathway is via the kidney. Collectively, our data suggest that Cr^{3+}

409   is capable of interfering extensively with shell calcification mechanisms.

410

411   To conclude, in extrapallial, hemolymph, heart and pericardium fluids of

412   *A. cygnea* it was observed that: (i) Mg^{2+} and, mainly, Ca^{2+} availability generally

413   revealed a rising trend following exposure to $Cu^{2+,}$ Cr^{3+} and Zn^{2+}, as a

414   consequence of the calcium microspherules dissolution in the gills and mantle,

415   whereas Na^+, Cl^- and K^+ contents decreased as a compensatory process in the

416   internal osmolarity regulation; (ii) Pb^{2+} exposure seems to affect calcium

417   absorption from the external medium in the epithelium separating the gut from

418   the heart; (iii) Cr^{3+} and Cu^{2+} affected nacreous layer formation in the shell,

419   whereas Pb^{2+} and Zn^{2+} appeared to have no influence on the shell structural

420   formation ; (iv) Zn^{2+} and, mainly, Cr^{3+} and Pb^{2+} accumulated in all

421   compartments sampled (extrapallial, hemolymph, heart and pericardium fluids

422   and kidney tissue), but Cu^{2+} exposure promoted a Cu^{2+} decrease in all

423   compartments except in the kidney, where it presumably accumulated for

424   excretion.

425 Finally, these results suggest that the essential metals $Cu^{2+,}$ and Zn^{2+} are

426 strongly regulated to remain at levels near the control, whereas the non-

427 essential metals Pb^{2+} and Cr^{3+} reach higher concentrations in all body

428 compartments, with apparent low or strong toxicity, respectively.

429

430

431

432

433 **Acknowledgements**

439

440

441 **References**

442 Antunes, C., Magalhães-Cardoso, T., Moura, G., Gonçalves, D., and Machado,

443   J. 2002. Effects of Al, Ni, Co, Zn, Cd and Cu metals on the outer mantle

444   epithelium of *Anodonta cygnea* (Unionidae). Haliotis, 31: 71-84

445 Audesirk, G. 1987. Effects of in vitro and in vivo lead exposure on voltage-

446   dependent calcium channels in central neurons of *Lymnaea stagnalis*.

447   Neuro Toxicology, 8: 579-592

448   Black, M.C., Ferrell, J.R., Horning, R.C. and Martin Jr., L.K. 1996. DNA strand
449   breakage in freshwater mussels *(Anodonta grandis)* exposed to lead in
450   the laboratory and field. Environ. Toxicol. Chem. 15 (5): 802–808.

451   Brown, P.L., Jeffree, R.A., and Markich, S.J. 1996. Kinetics of Ca-45, Co-60,
452   Pb-210, Mn-54 and Cd-109 in the tissue of the freshwater bivalve
453   *Velesunio angasi*: Further development of a predictive and mechanistic
454   model of metal bioaccumulation. Sci. Total Environ. 188: 139–166

455   Bryan, G.W. 1979. Bioaccumulation of marine pollutants. Philos. Trans. R. Soc.
456   Lond. B Biol. Sci. 286(1015): 483-505.

457   Bryan, G.W. 1971. The effects of heavy metals (other than mercury) on marine
458   and estuarine organisms. Proc. R. Soc. Lond. B. Biol. Sci. 177: 389-410

459   Choi, H.J., Ahn, I., Kim, K., Lee,Y., Lee, I., and Jeong, K. 2003. *Subcellular*
460   *accumulation of Cu in the Antarctic bivalve Laternula* elliptica from a
461   naturally Cu-elevated bay of King George Island. Polar Biol. 26: 601–609

462   Christensen, J.M., and Kristiansen, J. 1994. Lead. In Handbook on Metals *In*
463   Clinical and Analytical Chemistry. *Edited by* H. Seiler, A. Sigel and H.
464   Sigel. Marcel Dekker, New York. pp. 425-440

465   Calabrese, A., MacInnes, J.R., Nelson, D.A., and Miller, J.E. 1977. Survival and
466   growth of bivalve larvae under heavy-metal stress. Mar. Biol. (Berl.), 41:
467   179–184

468   Carriker, M.R., Palmer, R.E., Sick, L.V., and Johnson, C.C. 1980. Interaction of
469   mineral elements in sea water and shell of oysters (*Crassostrea virginica*
470   (Gmelin)) cultured in controlled and natural systems. J. Exp. Mar. Biol.
471   Ecol. 46: 279-296

472   Coimbra, J., Machado, J., Fernandes, P.L., Ferreira, H.G., and Ferreira, K.G.

473   1988. Electrophysiology of the mantle of *Anodonta cygnea*. J. Exp. Biol.

474   140: 65–88

475   Couillard, Y., Campbell, P.G.C., and Tessier, A. 1993 Response of

476   metallothionein concentrations in a freshwater bivalve (*Anodonta*

477   *grandis*) along an environmental cadmium gradient. Limnol. Oceanogr.

478   38: 299-313

479   Cross, C.E., Abrahim, A.B., Ahmed, M., and Mustafa, M.G. 1970. Effect of

480   cadmium ion on respiration and ATPase activity of the pulmonary

481   alveolar macrophage: a model for the study of the environmental

482   interference with pulmonary cell function. Environ. Res. 3: 512-520

483   Dallinger, R., and Wieser, W. 1984. Patterns of accumulation, distribution and

484   liberation of Zn, Cu, Cd and Pb in different organs of the land snail Helix

485   pomatia L. Comp. Biochem. Physiol. 79C(1): 117-124.

486   Faubel, D., Lopes-Lima, M., Freitas, S., Pereira, L., Andrade, J., Checa, A.,

487   Frank, H., Matsuda, T., and Machado, J. 2008. Effects of Cd^{2+} on the

488   Calcium Metabolism and Shell Mineralization of bivalve *Anodonta*

489   *cygnea*. Mar. Freshw. Behav. Phys. 41(2): 131-146.

490   Green, R.H. 1980. Role of a unionid clam population in the calcium budget of a

491   small arctic lake. Can. J. Fish. Aquat. Sci. 37: 219-224

492   Helfrich, L.A., Neves, R.J., Weigmann, D.L., Speenburgh, R.M., Beaty, B.B.,

493   Biggins, D., and Vinson. H. 1997. Help save America's pearly mussels.

494   Virginia Cooperative Extension Publication 420-014. Blacksburg,

495   Virginia. 16 pp.

496   Hemelraad, J., Holwerda, D.A., and Zandee, D.I. 1986. Cadmium kinetics in

497   freshwater clams. I. The pattern of cadmium accumulation in *Anodonta*

498   *cygnea.* Arch. Environ. Contam. Toxicol. 15: 9-21

499   Jeffree, R.A., Markich, S.J., and Brown, P.L. 1993 Comparative accumulation of

500   Alkaline-earth metals by two freshwater Mussel species from the Nepean

501   River, Australia: Consistencies and a resolved Paradox. Aust. J. Mar.

502   Fresh. Res. 44(4): 609-634

503   Jenner, H.A., Hemelraad, J., Marquenie, J.M., and Noppert, F. 1991. Cadmium

504   kinetics in freshwater clams (Unionidae) under field and laboratory

505   conditions. Sci. Total Environ. 108(3): 205-14

506   Jodrey, L.H. 1953. Studies on shell formation III. Measurement of calcium

507   deposition in shell and calcium turnover in mantle tissue using the

508   mantle-shell preparation and ^{45}Ca. Biol. Bull. Mar. 104: 398-407

509   Kado, Y. 1960. Studies on shell formation in molluscs. J. Sci. Hiroshima Univ.

510   Ser. B 19: 163-210

511   Katz, A.K., Glusker, J.P., Beebe, S.A., and Bock, C.W. 1996. Calcium ion

512   coordination: a comparison with that of beryllium, magnesium, and zinc.

513   J. Am. Chem. Soc. 118: 5752-5763.

514   Linde, A.R., Arribas, P., Sanchez-Galan, S., and Garcia-Vazquez, F. 1996. Eel

515   (*Anguilla anguilla*) and brown trout (*Salmo trutta*) target species to

516   assess the biological impact of trace metal pollution in freshwater

517   ecosystems. Arch. Environ. Contam. Toxicol. 31: 297-302

518   Lopes-Lima, M., Bleher, R., Forg, T., M Hafner, M. and Machado, J. 2008.

519   Studies on a PMCA-like protein in the outer mantle epithelium of

520   *Anodonta cygnea*: insights on calcium transcellular dynamics. *Journal of*

521   *ComparativePhysiology* 178(1):17-25

522   Lopes-Lima, M., Ribeiro, I., Pinto, R.A., and Machado, J. 2005. Isolation,

523   purification and characterization of glycosaminoglycans in the fluids of

524   the mollusc *Anodonta cygnea.* Comp. Biochem. Physiol. A 141: 319-326

525   Machado, J., Coimbra, J., Sá, C., and Cardoso, I. 1988. Shell thickening in

526   *Anodonta cygnea* by induced acidosis. Comp. Biochem. Physiol. A 91(4):

527   645-651

528   Machado, J. 1989. Estudos morfofuncionais da génese da concha de *Anodonta*

529   *cygnea.* PhD Thesis, Instituto de Ciências Biomédicas Abel Salazar,

530   Universidade do Porto, Porto, Portugal.

531   Machado, J., Reis, M.L., Coimbra, J., and Sá, C. 1991. Studies on chitin

532   calcification in the inner layers of the shell of Anodonta cygnea. J. Comp.

533   Physiol. 161:413-418

534   Manly, R., and George, W.O. 1977. The occurrence of some heavy metals in

535   populations of the freshwater mussel *Anodonta anatina* (L.) from the

536   River Thames. Environ. Pollut. 14: 139–154

537   Mason, A.Z., and Jenkins, K.D. 1995. Metal detoxification in aquatic organisms.

538   *In* Metal speciation and bioavailability in aquatic systems. *Edited by* A.

539   Tessier and D.R. Turner. Wiley, Chichester. pp. 479–608

540   Mason, A.Z., and Simkiss, K. 1982. Sites of mineral deposition in metal

541   accumulating cells. Exp. Cell Res. 139: 383-391.

542   McCall, P.L., Tevesz, M.S.J., and Schwelgien, S.F. 1979. Sediment mixing by

543   *Lampsilis radiata iliquoidea* (Mollusca) from western Lake Erie. J. Gt.

544   Lakes Res. 5: 105-111

545   Meites, L. 1964. Handbook of anaytical Chemistry. McGraw Hill, New York.

546   Mersh, J., Wagner, P., and Pihan, J.C. 1996. Copper in indigenous and

547   transplanted zebra mussels in relation to changing water concentrations

548   and body weight. Environ. Toxicol. Chem. 15(6): 866-893

549   Morton, B. 1983. Feeding and digestion in the Bivalvia. *In* The Mollusca Vol. 5

550   Physiology. *Edited by* K.M. Wilbur and A.S.M. Saleuddin, New York

551   Academic Press, New York pp. 65-147

552   Moura, G.M. 1999. "Estudo dos mecanismos de calcificação de um modelo

553   bivalve". PhD Thesis. Instituto de Ciências Biomédicas Abel Salazar,

554   Porto, Portugal

555   Moura, G., Guedes, R., and Machado, J. 1999. The extracellular mineral

556   concretions in *Anodonta cygnea* (L.): different types and manganese

557   exposure-caused changes. J. Shellfish Res. 18(2): 645–650

558   Moura, G., Vilarinho, L., Guedes, R., and Machado, J. 2000. The action of some

559   heavy metals on the calcification process of *Anodonta cygnea*

560   (Unionidae): nacre morphology and composition changes. Haliotis, 29:

561   43-53

562   Moura, G., Almeida, M.J., Machado, M.J., and Machado, J. 2001. Effects of

563   heavy metal exposure on ionic composition of fluids and nacre of

564   *Anodonta cygnea* (Unionidae). Haliotis, 30: 33-44

565   Moura, G., Almeida, M.J., Machado, M.J., Vilarinho, L., and Machado, J. 2003.

566   The action of environmental acidosis on the calcification process of

567   *Anodonta cygnea* (L.). Proceedings of the 8th International Symposium

568   on Biomineralization. Tokai Univ Press, Kanagawa, pp. 178-182

569 Moura, G., Coimbra, J. and Machado, J. 2004. Insights on nacre formation in

570   the freshwater clam, Anodonta cygnea (L.): An overview. Proceedings of

571   the 8th International Symposium on Biomineralization. Tokai Univ Press,

572   Kanagawa, pp. 129–132.

573 Naimo, T.J. 1995. A review of the effects of havy metals on freshwater mussels.

574   Ecotoxicology, 4: 341-362

575 Ngo, H.T.T., Gerstmann, S., and Frank, H. 2010*a*. Subchronic effects of

576   environment-like cadmium levels on the bivalve *Anodonta anatina*

577   (Linnaeus 1758): I. Bioaccumulation, distribution and effects on calcium

578   metabolism. Toxicol. Environ. Chem. Online published on 22 July 2010.

579   DOI: 10.1080/02772240802386049

580 Ngo, H.T.T., Gerstmann, S., and Frank, H. 2010*b*. Subchronic effects of

581   environment-like cadmium levels on the bivalve *Anodonta anatina*

582   (Linnaeus 1758): II. Effects on energy reserves in relation to calcium

583   metabolism. Toxicol. Environ. Chem. Online published on 23 July 2010.

584   DOI: 10.1080/02772240802503585

585 Ngo, H.T.T., Gerstmann, S., and Frank, H. 2010*c*. Subchronic effects of

586   environment-like cadmium levels on the bivalve *Anodonta anatina*

587   (Linnaeus 1758): III. Effects on carbonic anhydrase activity in relation to

588   calcium metabolism. Toxicol. Environ. Chem. Online published on 22

589   July 2010. DOI: 10.1080/02772240802503619

590 Nonnotte, L., Boitel, F., and Truchot, J.P. 1993. Waterbome copper causes gill

591   damage and hemolymph hypoxia in the shore crab *Carcinus maenas*

592   Can. J. Zool. 71:1569-1576

593   Nriagu, J.O. and Pacyna, J.M. 1988. Quantitative assessment of worldwide

594   contamination of air, water and soils by trace metals. Nature (London),

595   333: 134-139

596   Pietrzak, J.E., Bates, J.M., and Scott, R.M. 1976. Constituents of unionoid

597   extrapalial fluid II pH and metal ion composition. Hydrobiologia, 50(1):

598   89-93

599   Rtal, A., Nonnotte, L., and Truchot, J.P. 1996. Detoxification of exogenous

600   copper by binding to hemolymph proteins in the shore crab, *Carcinus*

601   *maenas.* Aquat. Toxicol. 36: 239-252

602   Rupert, E., Fox, R., and Barnes, R. 2003. Invertebrate Zoology: A Functional

603   Evolutionary Approach. Brooks Cole 7th Edition. 1008pp

604   Saeki, K., Okazaki, M., and Kubota, M. 1993. Heavy metal accumulation in a

605   semi-enclosed hypereutrophic system: Lake Teganuma, Japan. Water

606   Air Soil. Pollut. 69: 79-91

607   Salánki, J., Turpaev, T.M., and Nichaeva, M. 1991. Mussels as a test animal for

608   assessing environmental pollution and the sub-lethal effects of pollutants.

609   *In* Bioindicators and Environmental Management. *Edited by* D.W. Jeffrey

610   and B. Madden. Academic Press, London, pp. 235-244

611   Schoffeniels, E. 1951. Mise en evidence par l'utilisation de radio-calcium d'un

612   mecanisme d'absorption du calcium a partir du milieu exterieur chez

613   l'Anodonte. Arch. Int. Physiol. 58: 467-468

614   Simkiss, K. and Mason, A.Z. 1983 Metal ions: metabolic and toxic effects. *In*

615   The Mollusca Vol. 2. *Edited by* P.W. Hochachka. Academic Press, New

616   York, pp. 101-164.

617   Simons, T.J. 1986. Cellular interactions between lead and calcium. Br. Med.

618   Bull. 42: 431-434

619   S.-Rózsa, K., and Salánki, J. 1987. Excitable membranes – object of evaluating

620   the effect of heavy metals. Acta Biol. Hung. 38: 31-45

621   Van der Borght, O. 1963. Absorption directe du calcium et du strontium en

622   solution dans le milieu ambiant par un Gasteropode dulcicole: *Lymnata*

623   *stagnalis* (L.) Archs. Int. Physiol. Biochim. 71: 611-23

624   Van der Borght, O. 1963. In- and out-fluxes of calcium ions in freshwater

625   gasteropods. Archs. Int. Physiol. Biochim. 71: 46-50

626   Van der Borght, O., and Van Puymbroeck, S. 1964. Active transport of alkaline

627   earth ions as physiological base of the accumulation of some radio-

628   nuclides in freshwater molluscs. Nature (London), 204: 533-535

629   Van der Schalie, H., and Van der Schalie, A. 1950. The mussels of the

630   Mississipi River. Am. Midl. Nat. 44: 448-466

631   Westbroek, P. 1983. Biological metal accumulation and biomineralization in a

632   geological perspective. *In* Biomineralization and biological metal

633   accumulation. *Edited by* P. Westbroek and F.W. Jong. D. Reiner Publ.

634   Co. Dordrecht, Holland, pp. 1-11

635   Wilbur, K.M., and Jodrey, L. 1995. Studies on shell formation. V. the inhibition of

636   shell formation by carbonic anhydrase inhibitors. Biol. Bull. (Woods Hole)

637   108: 359-365.

638

639

640

641

642 **Captions**

643 **Figure 1**.

644 Calcium contents of fluid collected from anatomical compartments of *Anodonta*

645 *cygnea* L., 1758 and kidney tissue, after treatment with different heavy metals

646 (Cu, Zn, Pb, and Cr). Bars with superscripts differed significantly from untreated

647 controls (* *p*<0.05).

648

649 **Figure 2**.

650 Magnesium contents of fluid collected from anatomical compartments of

651 *Anodonta cygnea* L., 1758 and kidney tissue, after treatment with different

652 heavy metals (Cu, Zn, Pb and Cr). Bars with superscripts differed significantly

653 from untreated controls (* *p*<0.05).

654

655 **Figure 3.**

656 Potassium contents of fluid collected from anatomical compartments of

657 *Anodonta cygnea* L., 1758 and kidney tissue, after treatment with different

658 heavy metals (Cu, Zn, Pb and Cr). Bars with superscripts differed significantly

659 from untreated controls (* *p*<0.05).

660

661 **Figure 4.**

662 Sodium contents of fluid collected from anatomical compartments of *Anodonta*

663 *cygnea* L., 1758 and kidney tissue, after treatment with different heavy metals

664 (Cu, Zn, Pb and Cr). Bars with superscripts differed significantly from untreated

665 controls (* *p*<0.05).

666

667 **Figure 5.**

668 Chloride contents of fluid collected from anatomical compartments of *Anodonta*

669 *cygnea* L., 1758 and kidney tissue, after treatment with different heavy metals

670 (Cu, Zn, Pb and Cr). Bars with superscripts differed significantly from untreated

671 controls (* $p<0.05$).

672

673 **Figure 6.**

674 Osmolarity of fluid collected from anatomical compartments of *Anodonta cygnea*

675 L., 1758 and kidney tissue, after treatment with different heavy metals (Cu, Zn,

676 Pb and Cr). Bars with superscripts differed significantly from untreated controls

677 (* $p<0.05$).

678

679 **Figure 7.**

680 Copper ion content of fluid collected from anatomical compartments of

681 *Anodonta cygnea* L., 1758, after Cu treatment.

682

683 **Figure 8.**

684 Zinc ion content of fluid collected from anatomical compartments of *Anodonta*

685 *cygnea* L., 1758, after Zn treatment.

686

687 **Figure 9.**

688 Lead ion content of fluid collected from anatomical compartments of *Anodonta*

689 *cygnea* L., 1758, after Pb treatment. Bars with superscripts differed significantly

690 from controls (* $p<0.05$).

691

692   **Figure 10.**

693   Chromium ion content fluid collected from anatomical compartments of

694   *Anodonta cygnea* L., 1758, after Cr treatment. Bars with superscripts differed

695   significantly from controls (* $p<0.05$).

696
697   **Figure 11 (11.1-11.9).**

698   SEM images of the inner layer of a shell from a control *Anodonta cygnea* L.,

699   1758. The images are ordered from the exterior shell border to the interior.

700   **(11.1)** Shell border showing prismatic and nacreous layers. **(11.2)** Enhanced

701   image of the prismatic layer from the border. **(11.3)** Interface between the

702   prismatic and nacreous layers. **(11.4)** Beginning of the nacreous layer. **(11.5)**

703   Image of the interior nacreous layer from an intermediate location between the

704   border and the pallial line. **(11.6)** Nacreous layer just above the pallial line.

705   **(11.7)** The pallial line. **(11.8)** Beginning of the nacreous layer just below the

706   pallial line. (**11.9)** Nacreous layer interior of the pallial line.

707

708   **Figure 12 (12.1-12.4).**

709   SEM images of the inner layer of *Anodonta cygnea* L., 1758 shell from the Pb^{2+}

710   treatment group. The images are ordered from the exterior shell border to the

711   interior. **(12.1)** Shell border showing prismatic and nacreous layers. **(12.2)**

712   Beginning of the nacreous layer. **(12.3)** Nacreous layer just above the pallial

713   line. **(12.4)** Nacreous layer just below the pallial line.

714

715   **Figure 13 (13.1-13.4).**

716   SEM images of the inner layer of *Anodonta cygnea* L., 1758 shell from the Zn^{2+}

717   treatment group. The images are ordered from the exterior shell border to the

718   interior. **(13.1)** Shell border showing the prismatic and nacreous layer. (**13.2)**

719   Beginning of the nacreous layer. **(13.3)** Magnified nacreous layer. **(13.4)**

720   Nacreous layer just below the pallial line.

721

722   **Figure 14 (14.1-14.4).**

723   SEM images of the inner layer of *Anodonta cygnea* L., 1758 shell from the Cu^{2+}

724   treatment group. The images are ordered from the exterior shell border to the

725   interior. **(14.1)** Shell border showing the prismatic layer. **(14.2)** Beginning of the

726   nacreous layer. **(14.3)** Nacreous layer below the pallial line. **(14.4)** Magnification

727   of the same pallial region.

728

729   **Figure 15 (15.1-15.4).**

730   SEM images of the inner layer of *Anodonta cygnea* L., 1758 shell from the Cr^{3+}

731   treatment group. The images are ordered from the exterior shell border to the

732   interior. **(15.1)** Shell border showing the prismatic layer. **(15.2)** Beginning of the

733   nacreous layer. **(15.3)** Nacreous layer below the pallial line. **(15.4)** General view

734   of the nacreous layer below the pallial line.

735

736   **Figure 16 -** Diagram of ionic balance in *Anodonta cygnea* L., 1758, showing a

737   Ca^{2+} ion absorption and resorption from the gastrointestinal tract and

738   pericardium towards the ventricle compartment, respectively. Changes on the

739   osmolarity due to increased Ca^{2+} and Mg^{2+} under acidosis induced by Cu^{2+} or

740   Zn^{2+} and Cr^{3+} exposure. Whereas vitamin D is a stimulator of transepithelial

741   calcium   movements,   SEA0400   and Pb^{2+} are   specific   inhibitors   of

742 sodium/calcium ion exchange and calcium uptake in ventricle and

743 gastrointestinal tract epithelia, respectively.

744

745 **Figure 17**. - Circulatory and excretion system of bivalves diagram, showing a

746 circulatory pathway from the heart to the mantle and an excretion pathway from

747 the pericardium to the kidney through the reno-pericardial canal. Adapted from

748 (Rupert et al 2003).

749

Table 1 - Main ions concentration in samples of *A. cygnea* under Cu^{2+} exposure (1.0 x 10^{-6} M) for 30 days in the laboratory.

(C - control; E – experimental). ↑ significant increase (p<0,05), ↓ significant decrease (p<0,05).

	Extrapallial		Hemolymph		Heart		Pericardium		Kidney (mg/g)	
	C	E	C	E	C	E	C	E	C	E
Ca^{2+} (mmol/L)	11,49 ± 2,02	23,58 ± 6,81 ↑	9,91 ± 0,88	26,83 ± 2,90 ↑	13,38 ± 1,10	23,73 ± 3,68 ↑	11,45 ± 2,43	31,03 ± 5,79 ↑	4,25 ± 0,38	3,88 ± 1,29
Mg^{2+} (µmol/L)	31,13 ± 3,88	45,38 ± 17,17	23,50 ± 1,80	44,63 ± 12,69 ↑	28,33 ± 5,32	55,98 ± 6,45 ↑	34,75 ± 1,55	58,98 ± 9,98 ↑	0,45 ± 0,003	0,36 ± 0,08
K^{+} (µmol/L)	262,50 ± 55,20	200,25 ± 47,00	217,75 ± 25,57	216,00 ± 24,00	257,00 ± 61,10	220,25 ± 65,31	293,00 ± 25,10	223,00 ± 49,90	0,81 ± 0,16	0,554 ± 0,10
Na^{+} (mmol/L)	8,97 ± 0,64	2,54 ± 0,51 ↓	8,77 ± 2,17	3,07 ± 0,71 ↓	8,94 ± 0,66	2,56 ± 0,36 ↓	8,67 ± 0,84	2,59 ± 0,73 ↓	2,04 ± 0,14	0,46 ± 0,16 ↓
Cl^{-} (mmol/L)	15,00 ± 1,80	7,75 ± 0,50 ↓	15,00 ± 3,70	8,75 ± 1,26 ↓	16,25 ± 1,71	8,75 ± 0,50 ↓	15,25 ± 1,50	11,25 ± 0,50 ↓		
Osmolality (mosm/L)	37,25 ± 2,99	24,75 ± 7,09 ↓	41,75 ± 17,21	27,25 ± 2,99	40,00 ± 0,80	34,00 ± 3,60 ↓	39,50 ± 1,90	34,50 ± 2,90 ↓		

Table 2 - Main ions concentration in samples of *A. cygnea* under Zn^{2+} exposure (1.0 x 10^{-6} M) for 30 days in the laboratory.

C - control; E – experimental; ↑ significant increase (p<0,05), ↓ significant decrease (p<0,05).

|	Extrapallial		Hemolymph		Heart		Pericardium		Kidney (mg/g)	
	C	E	C	E	C	E	C	E	C	E
Ca^{2+} (mmol/L)	11,49 ± 2,02	15,43 ± 0,47 ↑	9,91 ± 0,88	13,70 ± 2,40 ↑	13,38 ± 1,10	15,70 ± 1,10 ↑	11,45 ± 2,43	15,23 ± 1,32 ↑	4,25 ± 0,38	2,87 ± 0,72
Mg^{2+} (µmol/L)	31,13 ± 3,88	38,00 ± 7,80	23,50 ± 1,80	33,03 ± 9,46	28,33 ± 5,32	34,00 ± 9,50	34,75 ± 1,55	40,55 ± 5,28	0,45 ± 0,003	0,26 ± 0,12
K^{+} (µmol/L)	262,50 ± 55,20	236,75 ± 37,58	217,75 ± 25,57	211,75 ± 39,96	257,00 ± 61,10	200,75 ± 30,84	293,00 ± 25,10	228,25 ± 25,60 ↓	0,81 ± 0,16	0,54 ± 0,22
Na^{+} (mmol/L)	8,97 ± 0,64	8,51 ± 0,47	8,77 ± 2,17	7,59 ± 0,69	8,94 ± 0,66	8,27 ± 0,54	8,67 ± 0,84	7,88 ± 0,67	2,04 ± 0,14	1,33 ± 0,88
Cl^{-} (mmol/L)	15,00 ± 1,80	13,75 ± 0,50	15,00 ± 3,70	13,25 ± 0,50	16,25 ± 1,71	12,25 ± 0,50 ↓	15,25 ± 1,50	12,75 ± 0,50 ↓		
Osmolality (mosm/L)	37,25 ± 2,99	38,75 ± 3,40	41,75 ± 17,21	33,25 ± 7,37	40,00 ± 0,80	35,25 ± 2,63 ↓	39,50 ± 1,90	37,25 ± 1,26		

Table 3 - Main ions concentration in samples of *A. cygnea* under Cr^{3+} exposure (1.0×10^{-6} M) for 30 days in the laboratory.

C - control; E – experimental; ↑ significant increase (p<0,05), ↓ significant decrease (p<0,05).

	Extrapallial		Hemolymph		Heart		Pericardium		Kidney (mg/g)	
	C	E	C	E	C	E	C	E	**C**	**E**
Ca²⁺ (mmol/L)	11,49 ± 2,02	17,30 ± 3,30 ↑	9,91 ± 0,88	14,90 ± 3,90	13,38 ± 1,10	15,70 ± 3,40	11,45 ± 2,43	19,50 ± 4,90 ↑	4,25 ± 0,38	4,99 ± 1,53
Mg²⁺ (µmol/L)	31,13 ± 3,88	46,03 ± 4,87 ↑	23,50 ± 1,80	47,48 ± 9,99 ↑	28,33 ± 5,32	46,03 ± 4,87 ↑	34,75 ± 1,55	59,20 ± 10,80 ↑	0,45 ± 0,003	0,53 ± 0,23
K⁺ (µmol/L)	262,50 ± 55,20	168,00 ± 33,90 ↓	217,75 ± 25,57	180,25 ± 39,78	257,00 ± 61,10	168,00 ± 33,90	293,00 ± 25,10	205,50 ± 18,40 ↓	0,81 ± 0,16	0,86 ± 0,43
Na⁺ (mmol/L)	8,97 ± 0,64	5,60 ± 0,70 ↓	8,77 ± 2,17	6,31 ± 1,08	8,94 ± 0,66	5,60 ± 0,70 ↓	8,67 ± 0,84	5,93 ± 0,64 ↓	2,04 ± 0,14	1,83 ± 0,97
Cl⁻ (mmol/L)	15,00 ± 1,80	9,00 ± 0,80 ↓	15,00 ± 3,70	8,75 ± 0,50 ↓	16,25 ± 1,71	9,00 ± 0,80 ↓	15,25 ± 1,50	7,50 ± 0,60 ↓		
Osmolality (mosm/L)	37,25 ± 2,99	16,75 ± 1,5 ↓	41,75 ± 17,21	19,50 ± 2,10 ↓	40,00 ± 0,80	25,00 ± 2,80 ↓	39,50 ± 1,90	25,25 ± 1,89 ↓		

Table 4 - Main ions concentration in samples of *A. cygnea* under Pb^{2+} exposure (1.0×10^{-6} M) for 30 days in the laboratory.

C - control; E – experimental; ↑ significant increase ($p<0,05$), ↓ significant decrease ($p<0,05$).

	Extrapallial		Hemolymph		Heart		Pericardium		Kidney (mg/g)	
	C	E	C	E	C	E	C	E	C	E
Ca^{2+} (mmol/L)	11,49 ± 2,02	12,34 ± 2,23	9,91 ± 0,88	8,57 ± 1,45	13,38 ± 1,10	9,71 ± 1,20 ↓	11,45 ± 2,43	11,56 ± 2,21	4,25 ± 0,38	3,57 ± 0,22
Mg^{2+} (µmol/L)	31,13 ± 3,88	35,68 ± 5,51	23,50 ± 1,80	28,68 ± 2,41 ↑	28,33 ± 5,32	29,73 ± 5,08	34,75 ± 1,55	41,43 ± 3,19 ↑	0,45 ± 0,003	0,392 ± 0,05
K^{+} (µmol/L)	262,50 ± 55,20	80,55 ± 33,45 ↓	217,75 ± 25,57	46,58 ± 32,34 ↓	257,00 ± 61,10	53,60 ± 29,70 ↓	293,00 ± 25,10	103,03 ± 31,60 ↓	0,81 ± 0,16	0,50 ± 0,08
Na^{+} (mmol/L)	8,97 ± 0,64	5,85 ± 0,35 ↓	8,77 ± 2,17	5,87 ± 0,30 ↓	8,94 ± 0,66	5,97 ± 0,37 ↓	8,67 ± 0,84	5,49 ± 0,29 ↓	2,04 ± 0,14	0,99 ± 0,06
Cl^{-} (mmol/L)	15,00 ± 1,80	10,25 ± 0,50 ↓	15,00 ± 3,70	10,50 ± 1,30	16,25 ± 1,71	10,00 ± 0,80 ↓	15,25 ± 1,50	10,50 ± 1,3 ↓		
Osmolality (mosm/L)	37,25 ± 2,99	37,50 ± 15,40	41,75 ± 17,21	27,25 ± 7,37	40,00 ± 0,80	41,75 ± 5,12	39,50 ± 1,90	33,25 ± 4,19		

Table 5 - Metal ion concentration in the samples under the respective metal exposure at a sub-lethal concentration (1.0×10^{-6} M) for 30 days in the laboratory.

(C - control; E – experimental) ↑ significant increase ($p<0,05$), ↓ significant decrease ($p<0,05$), n.d. (not detected).

|	Extrapallial		Hemolymph		Heart		Pericardium		Kidney (mg/g)	
	C	**E**	**C**	**E**	**C**	**E**	**C**	**E**	**C**	**E**
Cu^{2+} (µmol/L)	0,85 ± 0,18	0,67 ± 0,22	0,82 ± 0,20	0,47 ± 0,29	0,98 ± 0,22	0,73 ± 0,27	0,89 ± 0,29	0,63 ± 0,36	55,20 ± 20,00	83,73 ± 25,36
Zn^{2+} (µmol/L)	1,90 ± 0,40	2,91 ± 1,96	2,55 ± 0,67	3,99 ± 3,37	2,36 ± 0,70	4,60 ± 1,18	2,90 ± 0,80	3,36 ± 1,59	0,13 ± 0,03	0,12 ± 0,006
Cr^{3+} (nmol/L)	n.d.	61,45 ± 15,05 ↑	n.d.	54,73 ± 12,32 ↑	n.d.	61,45 ± 15,05 ↑	n.d.	214,00 ± 42,10 ↑	0,90 ± 0,44	29,84 ± 13,92 ↑
Pb^{2+} (nmol/L)	24,30 ± 5,30	739,00 ± 430,80 ↑	24,63 ± 5,01	858,00 ± 458,00 ↑	25,68 ± 3,63	859,50 ± 501,70 ↑	26,03 ± 13,40	331,75 ± 192,65	4,12 ± 0,96	34,12 ± 12,67 ↑
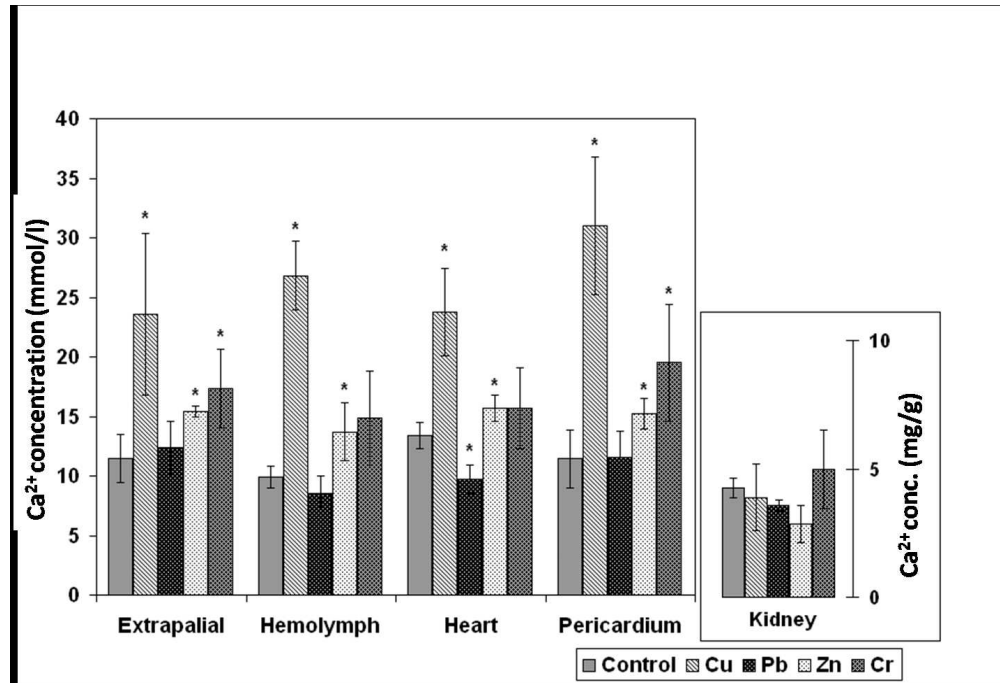
Calcium contents of fluid collected from anatomical compartments of Anodonta cygnea L., 1758 and kidney tissue, after treatment with different heavy metals (Cu, Zn, Pb, and Cr). Bars with superscripts differed significantly from untreated controls (* $p<0.05$).
242x165mm (150 x 150 DPI)
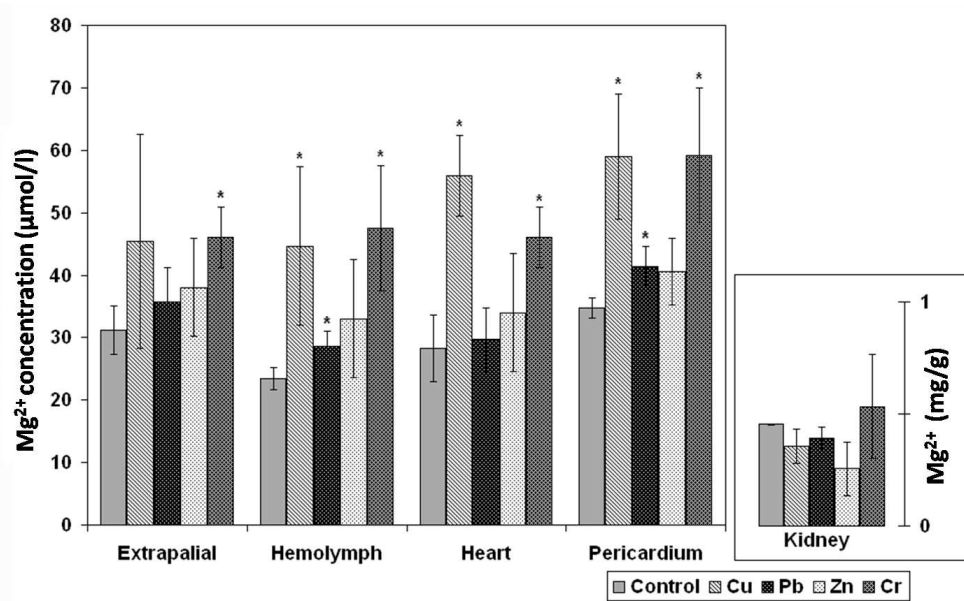
Magnesium contents of fluid collected from anatomical compartments of Anodonta cygnea L., 1758 and kidney tissue, after treatment with different heavy metals (Cu, Zn, Pb and Cr). Bars with superscripts differed significantly from untreated controls (* p<0.05).
242x147mm (150 x 150 DPI)
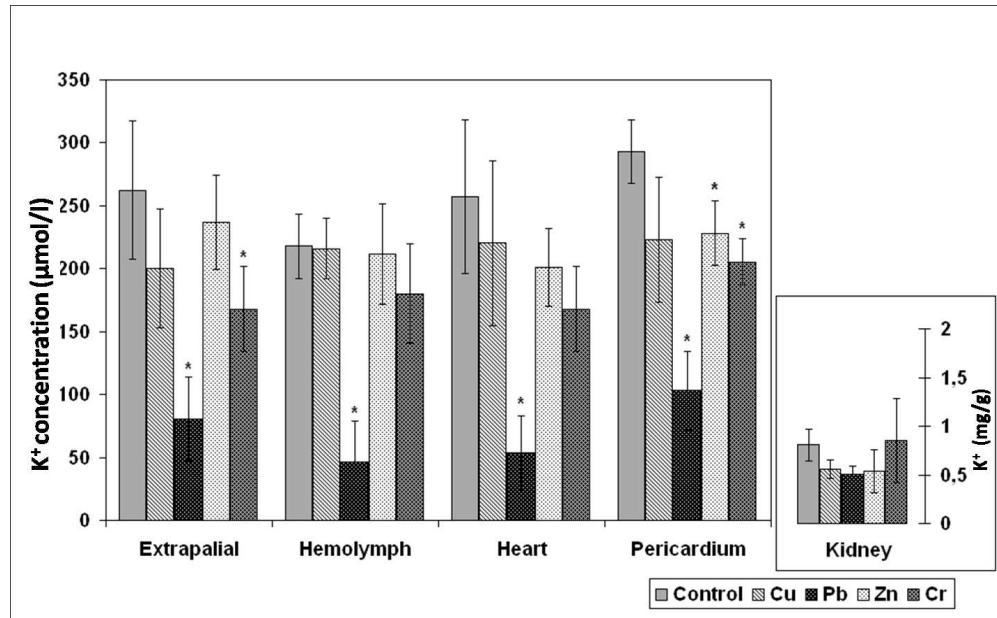
Potassium contents of fluid collected from anatomical compartments of Anodonta cygnea L., 1758 and kidney tissue, after treatment with different heavy metals (Cu, Zn, Pb and Cr). Bars with superscripts differed significantly from untreated controls (* p<0.05).
242x149mm (150 x 150 DPI)
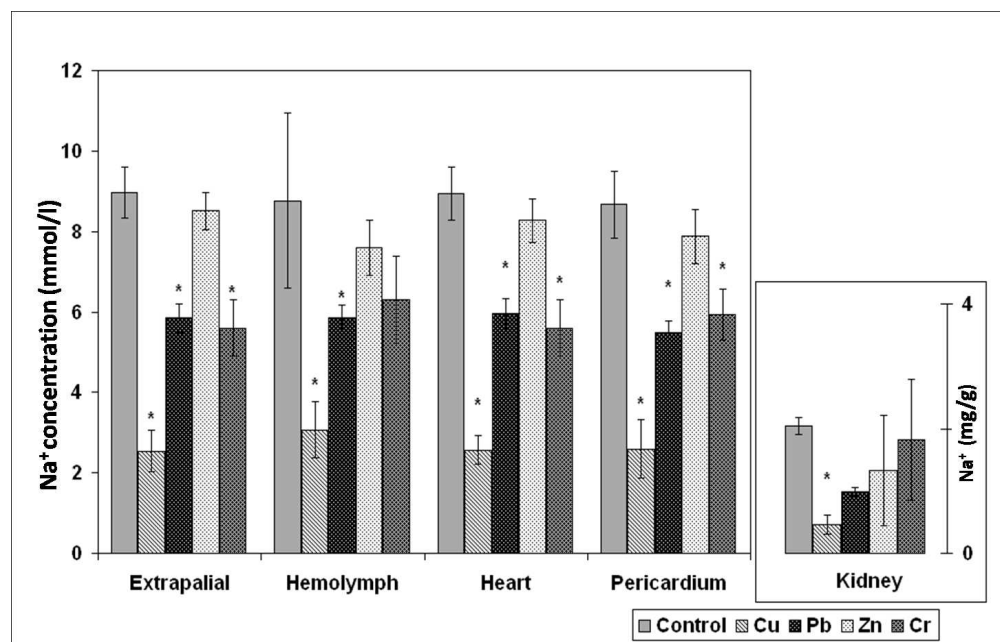
Sodium contents of fluid collected from anatomical compartments of Anodonta cygnea L., 1758 and kidney tissue, after treatment with different heavy metals (Cu, Zn, Pb and Cr). Bars with superscripts differed significantly from untreated controls (* p<0.05).
246x157mm (150 x 150 DPI)
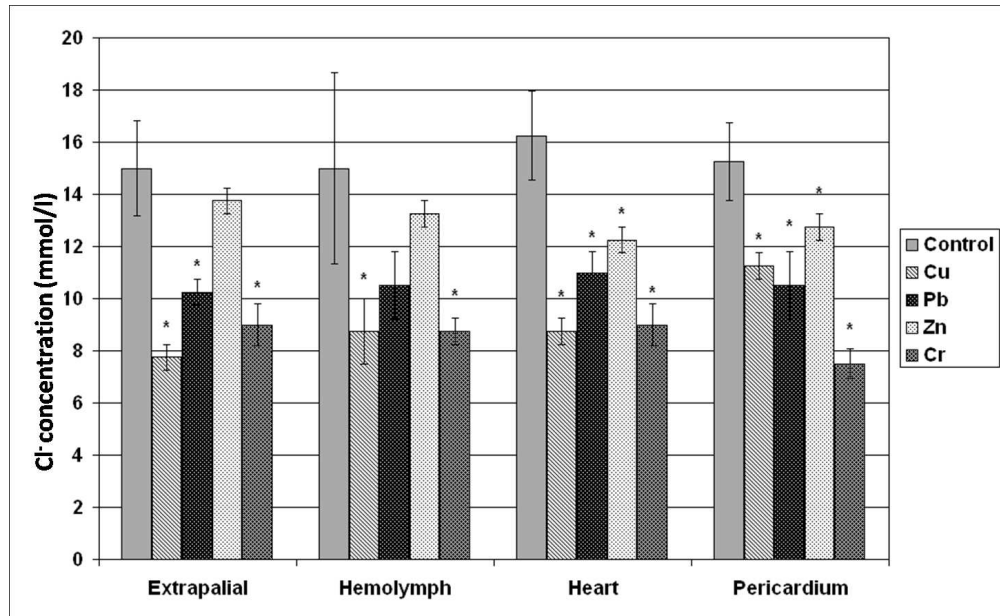
Chloride contents of fluid collected from anatomical compartments of Anodonta cygnea L., 1758 and kidney tissue, after treatment with different heavy metals (Cu, Zn, Pb and Cr). Bars with superscripts differed significantly from untreated controls (* p<0.05).
245x151mm (150 x 150 DPI)
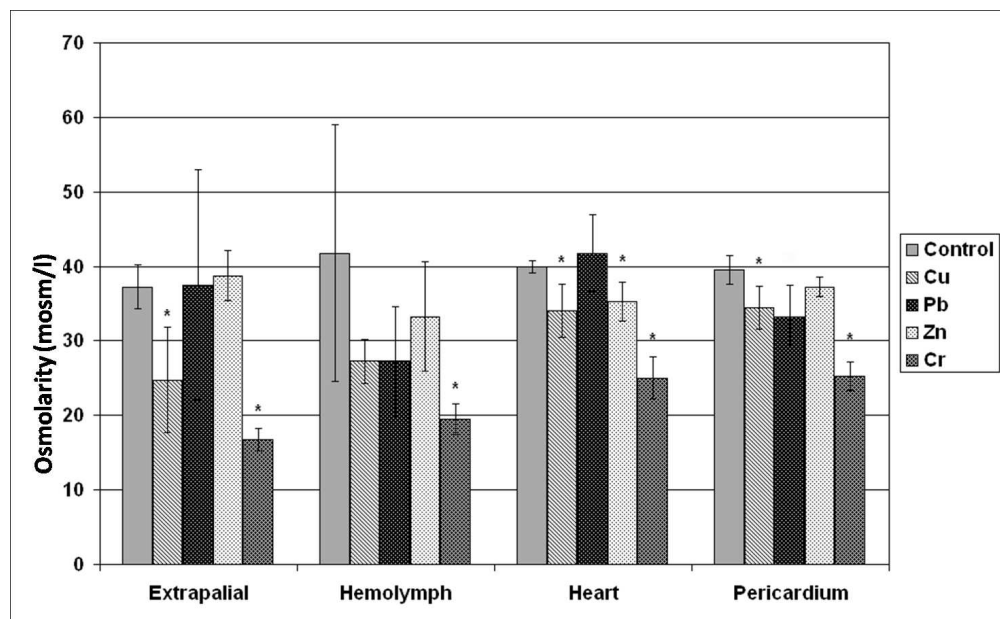
Osmolarity of fluid collected from anatomical compartments of Anodonta cygnea L., 1758 and kidney tissue, after treatment with different heavy metals (Cu, Zn, Pb and Cr). Bars with superscripts differed significantly from untreated controls (* p<0.05).
249x153mm (150 x 150 DPI)
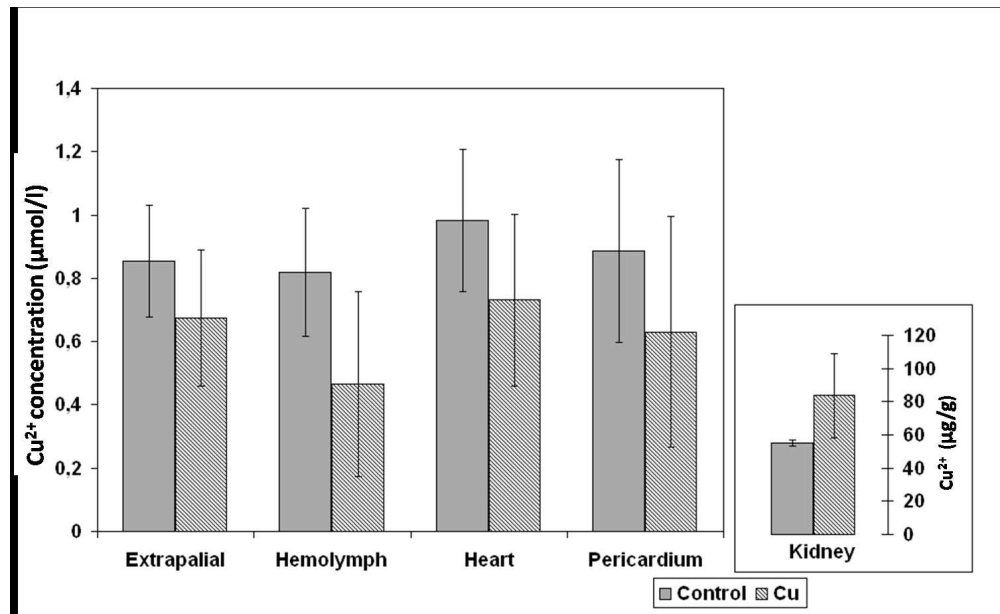
Copper ion content of fluid collected from anatomical compartments of Anodonta cygnea L., 1758, after Cu treatment.
255x155mm (150 x 150 DPI)
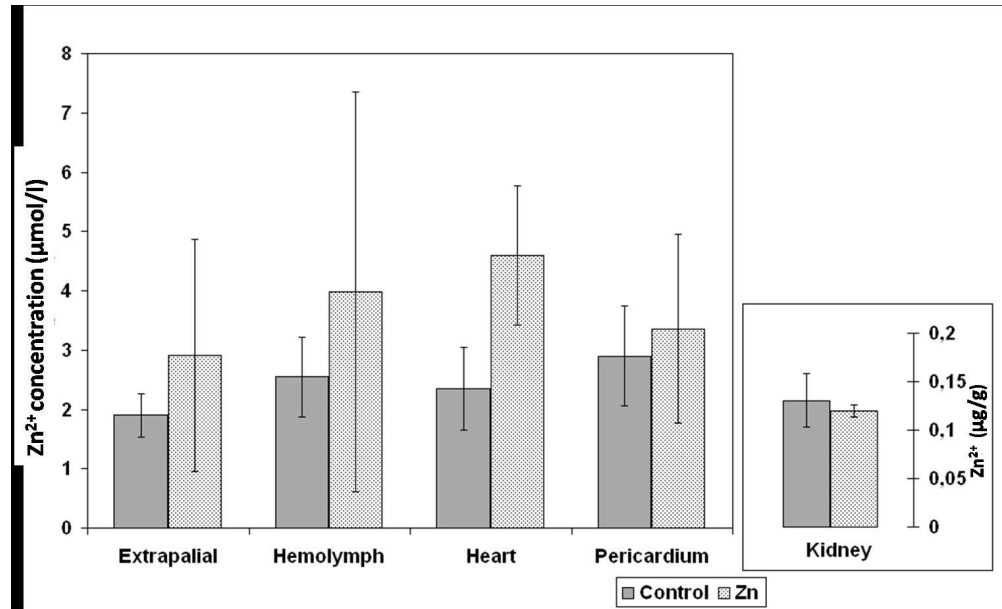
Zinc ion content of fluid collected from anatomical compartments of Anodonta cygnea L., 1758, after Zn treatment.
257x156mm (150 x 150 DPI)
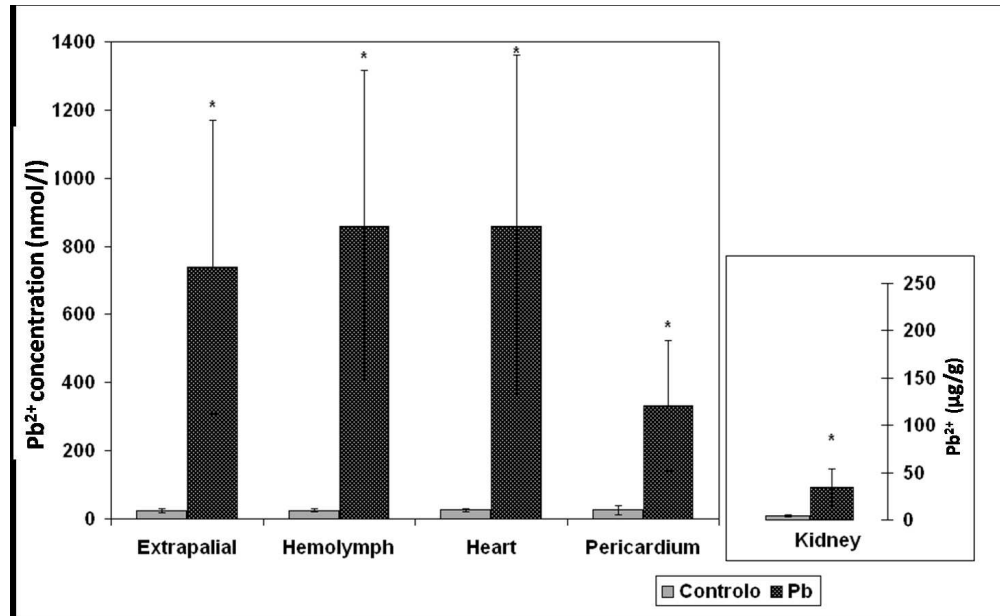
Lead ion content of fluid collected from anatomical compartments of Anodonta cygnea L., 1758, after Pb treatment. Bars with superscripts differed significantly from controls (* $p < 0.05$).
247x151mm (150 x 150 DPI)
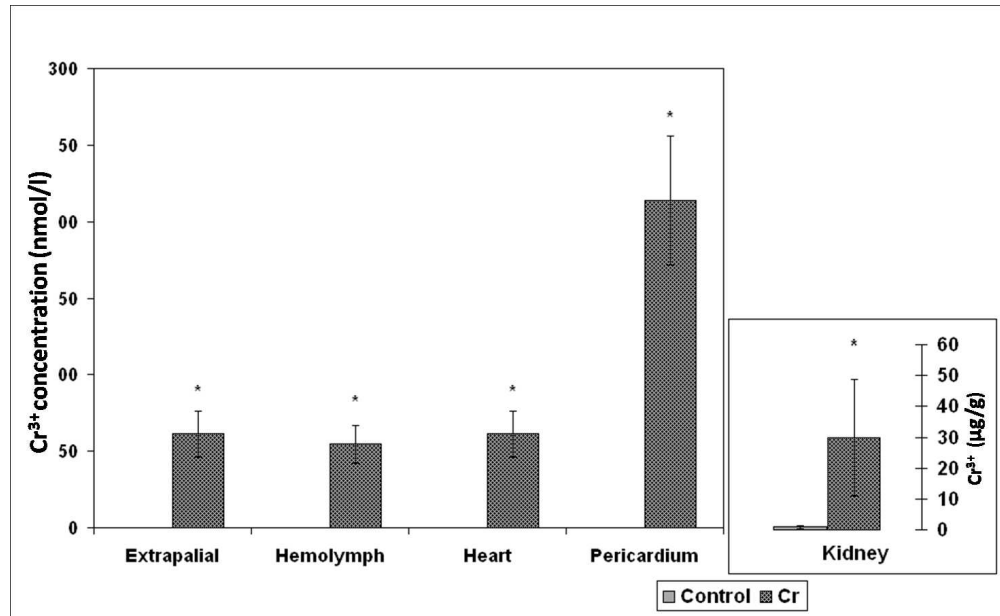
Chromium ion content fluid collected from anatomical compartments of Anodonta cygnea L., 1758, after Cr treatment. Bars with superscripts differed significantly from controls (* p<0.05).
249x153mm (150 x 150 DPI)
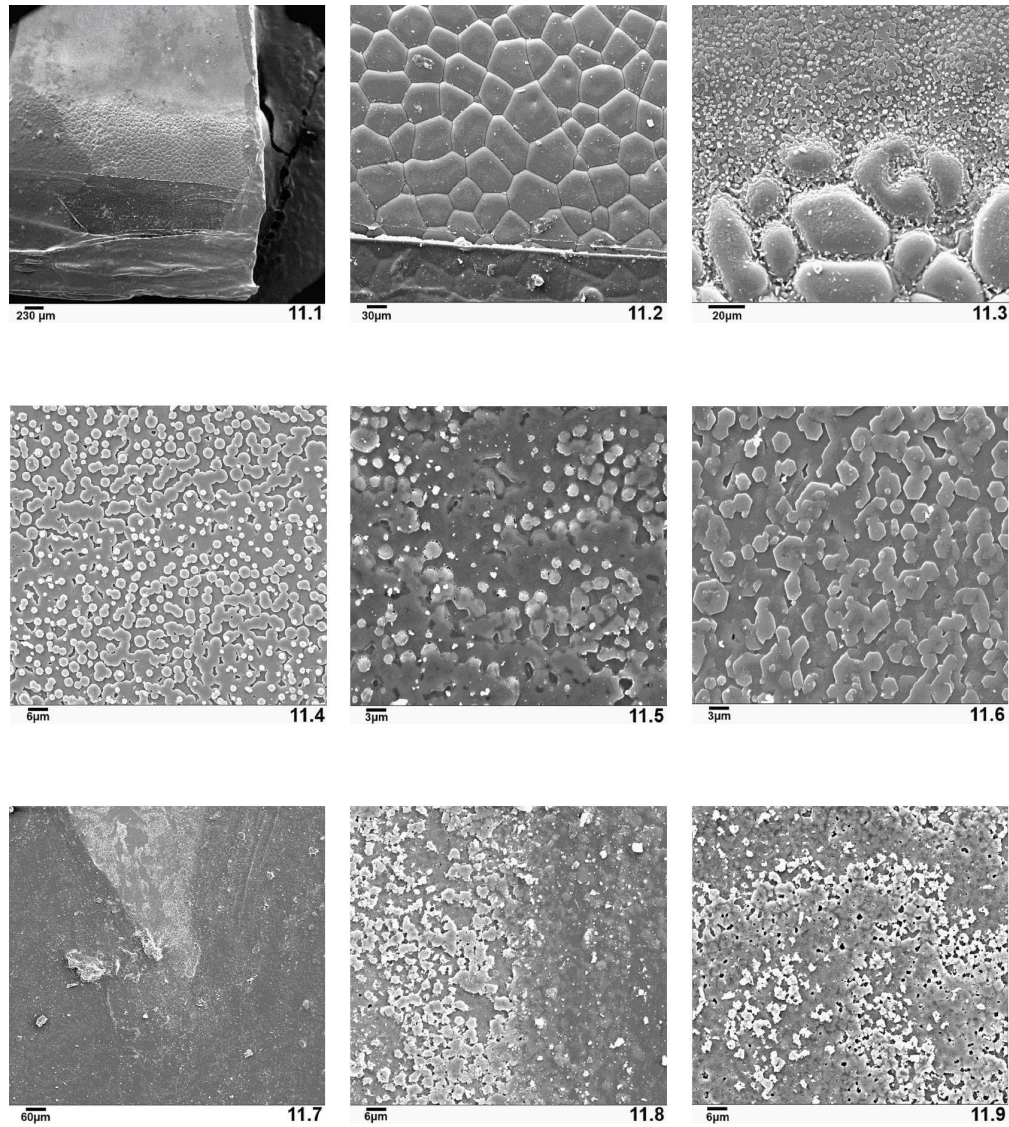
SEM images of the inner layer of a shell from a control Anodonta cygnea L., 1758. The images are ordered from the exterior shell border to the interior. (11.1) Shell border showing prismatic and nacreous layers. (11.2) Enhanced image of the prismatic layer from the border. (11.3) Interface between the prismatic and nacreous layers. (11.4) Beginning of the nacreous layer. (11.5) Image of the interior nacreous layer from an intermediate location between the border and the pallial line. (11.6) Nacreous layer just above the pallial line. (11.7) The pallial line. (11.8) Beginning of the nacreous layer just below the pallial line. (11.9) Nacreous layer interior of the pallial line.
884x989mm (96 x 96 DPI)
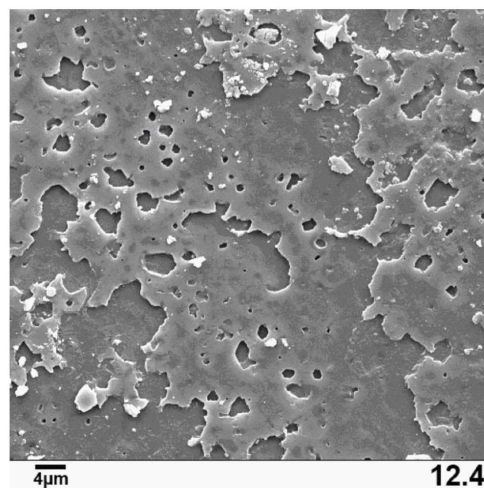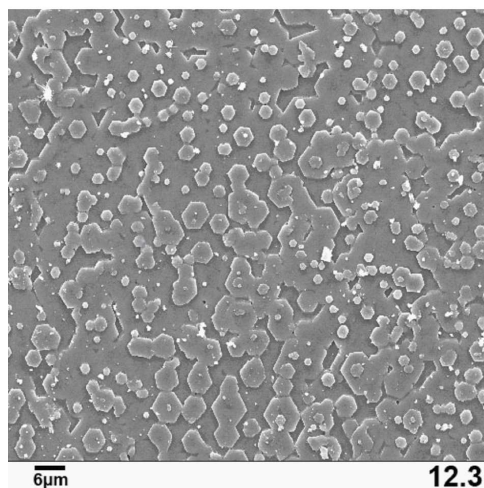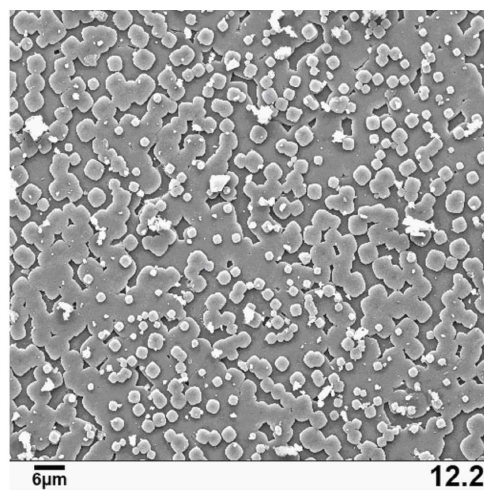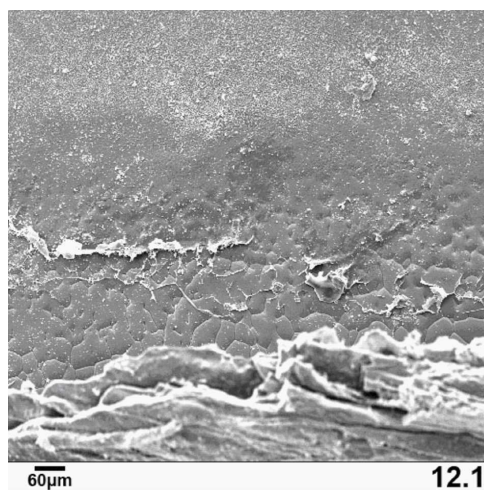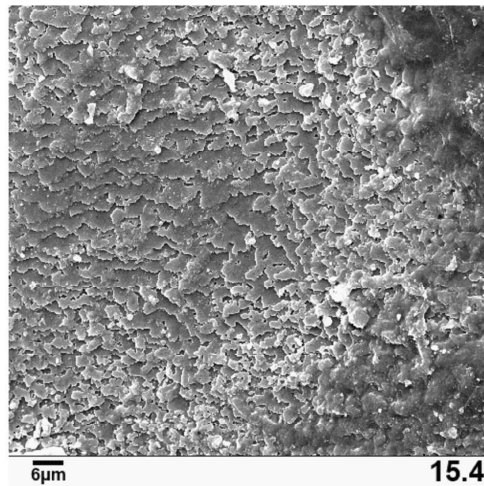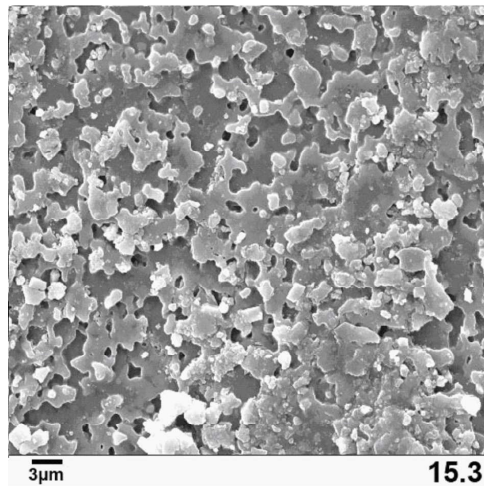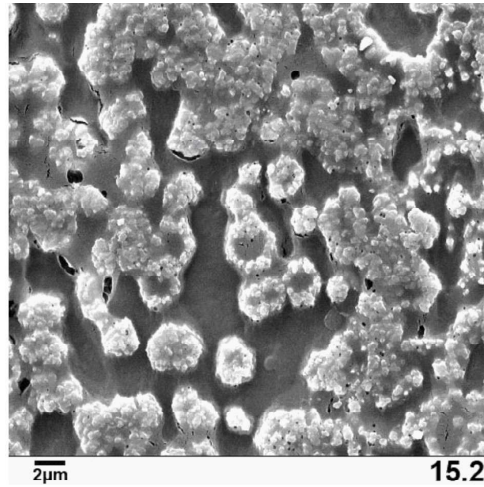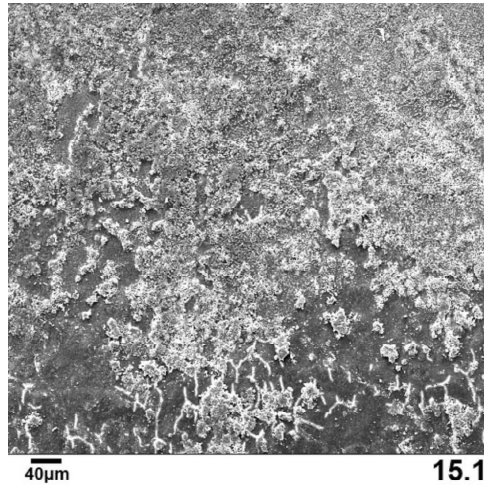
SEM images of the inner layer of Anodonta cygnea L., 1758 shell from the Pb2+ treatment group. The images are ordered from the exterior shell border to the interior. (12.1) Shell border showing prismatic and nacreous layers. (12.2) Beginning of the nacreous layer. (12.3) Nacreous layer just above the pallial line. (12.4) Nacreous layer just below the pallial line.
1039x1126mm (96 x 96 DPI)
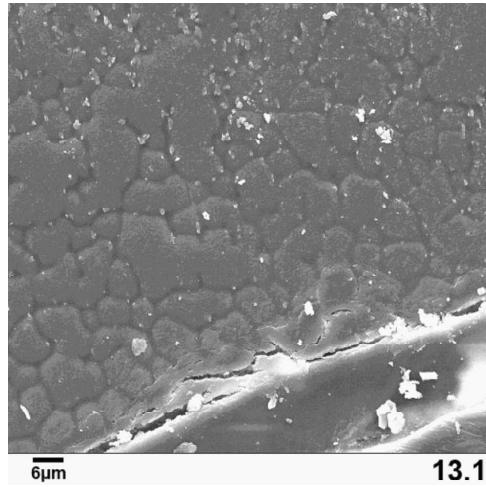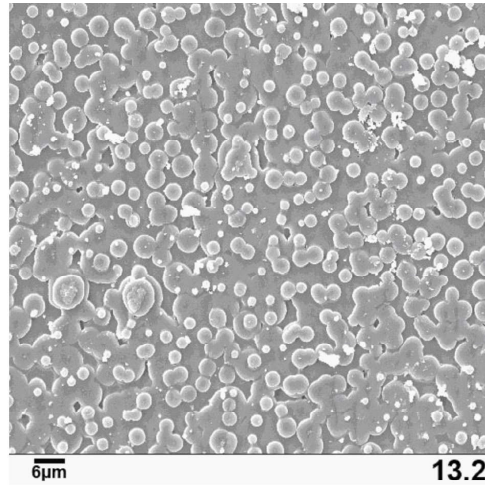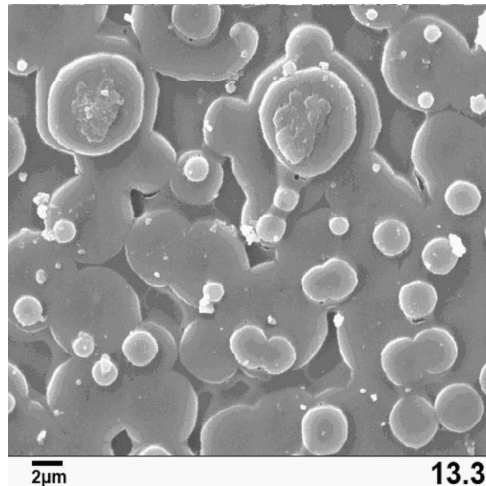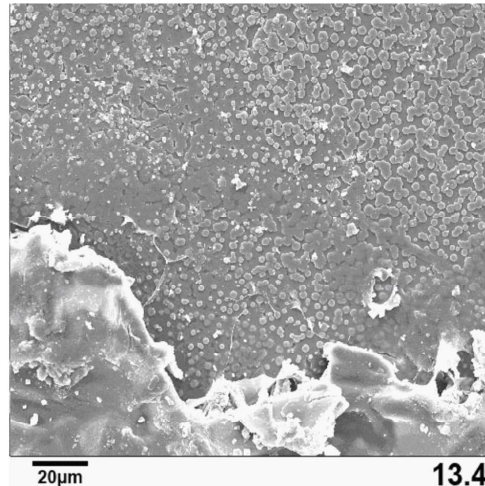
SEM images of the inner layer of Anodonta cygnea L., 1758 shell from the Zn2+ treatment group. The images are ordered from the exterior shell border to the interior. (13.1) Shell border showing the prismatic and nacreous layer. (13.2) Beginning of the nacreous layer. (13.3) Magnified nacreous layer. (13.4) Nacreous layer just below the pallial line.
1034x1127mm (96 x 96 DPI)
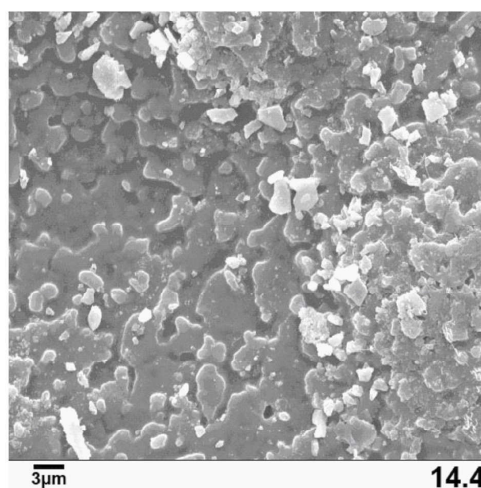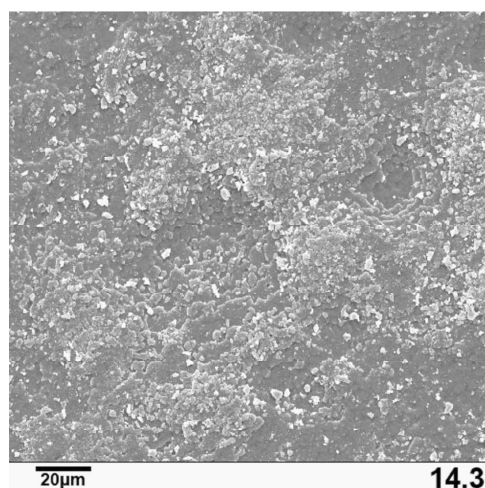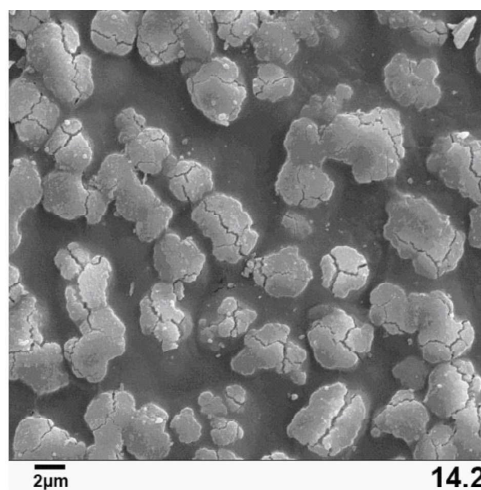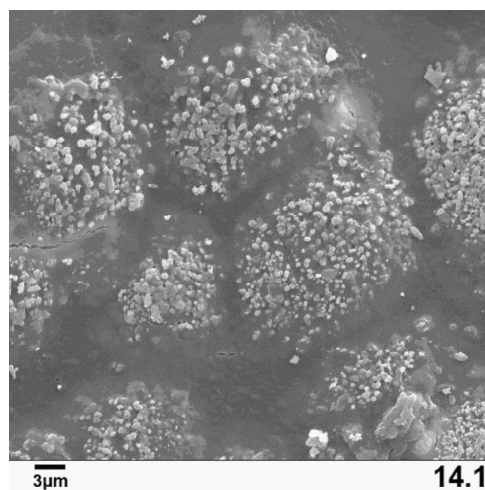
SEM images of the inner layer of Anodonta cygnea L., 1758 shell from the Cu2+ treatment group. The images are ordered from the exterior shell border to the interior. (14.1) Shell border showing the prismatic layer. (14.2) Beginning of the nacreous layer. (14.3) Nacreous layer below the pallial line. (14.4) Magnification of the same pallial region.
1036x1126mm (96 x 96 DPI)

SEM images of the inner layer of Anodonta cygnea L., 1758 shell from the Cr3+ treatment group. The images are ordered from the exterior shell border to the interior. (15.1) Shell border showing the prismatic layer. (15.2) Beginning of the nacreous layer. (15.3) Nacreous layer below the pallial line. (15.4) General view of the nacreous layer below the pallial line.
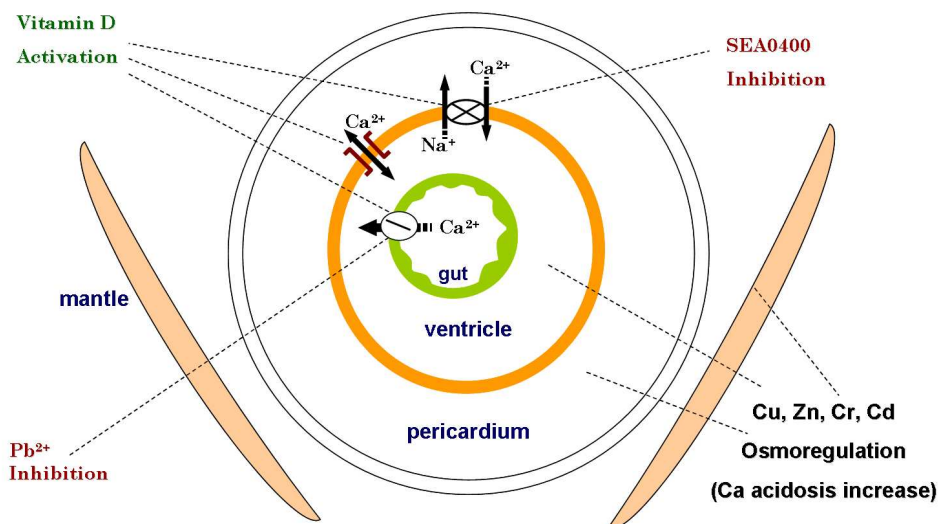1036x1126mm (96 x 96 DPI)

Diagram of ionic balance in Anodonta cygnea L., 1758, showing a Ca2+ ion absorption and resorption from the gastrointestinal tract and pericardium towards the ventricle compartment, respectively. Changes on the osmolarity due to increased Ca2+ and Mg2+ under acidosis induced by Cu2+ or Zn2+ and Cr3+ exposure. Whereas vitamin D is a stimulator of transepithelial calcium movements, SEA0400 and Pb2+ are specific inhibitors of sodium/calcium ion exchange and calcium uptake in ventricle and gastrointestinal tract epithelia, respectively.

273x145mm (144 x 144 DPI)
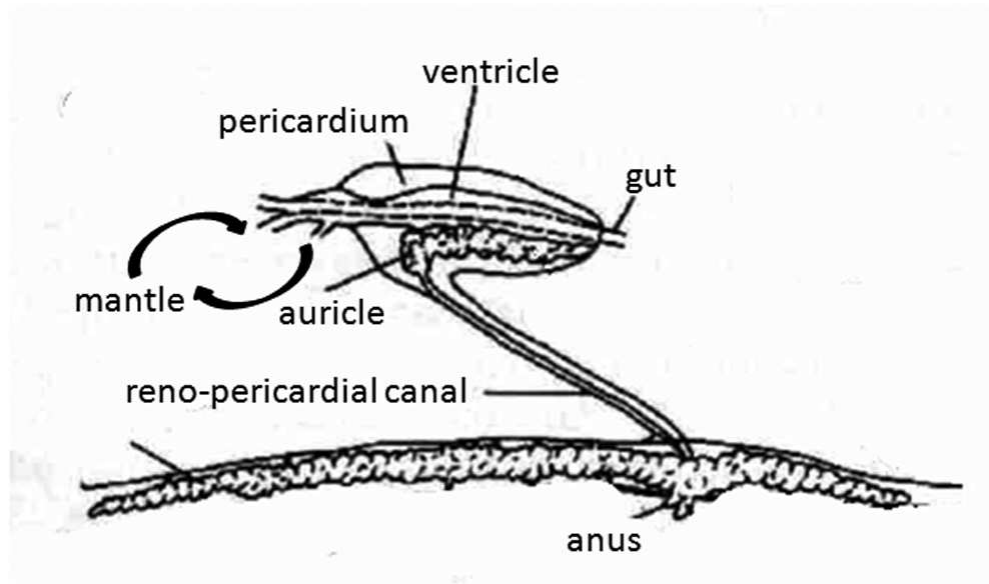
Circulatory and excretion system of bivalves diagram, showing a circulatory pathway from the heart
to the mantle and an excretion pathway from the pericardium to the kidney through the reno-
pericardial canal. Adapted from (Rupert et al 2003).
352x206mm (72 x 72 DPI)